



3D Geomodeling for Europe
Project number: GeoE.171.005

Deliverable 4.2

Sources of uncertainty in 3D geomodels

Main-Authors and affiliation:
Björn Zehner, Conxi Ayala, Frithjof Bense, Willem Dabekaussen, Maryke den Dulk, Jan Franek, Emilio L. Pueyo, Alexander Malz, Christian Olaf Müller, Heidrun Stück

[BGR][TNO][LAGB][CGS][IGME]

E-mail of lead author:
Bjoern.Zehner@bgr.de

Version: 02.09.2021

This report is part of a project that has received funding by the European Union’s Horizon 2020 research and innovation programme under grant agreement number 731166.



Deliverable Data		
Deliverable number	D4.2	
Dissemination level	Public	
Deliverable name	Report on the sources of uncertainty in 3D geomodels	
Work package	WP4, Uncertainty in Geomodels	
Lead WP/Deliverable beneficiary	BGR	
Deliverable status		
Submitted (Lead Author)	02/09/2021	Björn Zehner
Verified (WP leader)	02/09/2021	Björn Zehner
Approved (Project Leader)	03/09/2021	Stefan Knopf

Many of the sections of this document have been written primarily by specific groups of authors from the different project partners (Geological Survey Organizations / GSOs):

- BGR Bundesanstalt für Geowissenschaften und Rohstoffe - Federal Institute for Geosciences and Natural Resources, Germany
- CGS Česká geologická služba - Czech Geological Survey
- IGME Instituto Geológico y Minero de España – Geological Survey of Spain
- LAGB Landesamt für Geologie und Bergwesen – Geological Survey of Saxony-Anhalt, Germany
- TNO TNO - Geological Survey of the Netherlands

Section	GSO	Contributors
1	BGR	Björn Zehner
2		
2.1	BGR	Björn Zehner
2.2.1 – 2.2.3	LAGB	Christian Olaf Müller
2.2.4	BGR	Björn Zehner
2.2.5	LAGB	Alexander Malz
2.3	BGR	Björn Zehner
2.3.1	BGR	Björn Zehner
2.3.2	BGR	Björn Zehner, Frithjof Bense
2.3.3	BGR	Frithjof Bense, Heidrun Stück, Fabian Jähne-Klingberg
2.3.4	TNO	Maryke den Dulk
2.4	IGME	Emilio Pueyo, Conxi Ayala, Félix Rubio, Esther Izquierdo, Ruth Soto, Pablo Santolaria, Pilar Clariana, Carmen Rey
2.5	BGR	Björn Zehner
3		
3.1	BGR	Björn Zehner
3.2	TNO	Maryke den Dulk
3.3	TNO	Willem Dabekaussen
3.4	CGS	Jan Franěk, František Staněk, Jan Jelínek
4	BGR	Björn Zehner

Further we thank Ines Görz, Geological Survey of Saxony, and Alison E. Martin, JGU Mainz/Germersheim for reviewing and proof reading the manuscript.

GENERAL INTRODUCTION

When 3D models of the geological subsurface are built on a large scale, for example on basin scale, they are usually based on data such as seismic and borehole measurements and on field records which often involve a considerable amount of uncertainty. This can be, but is not limited to, measurement imprecisions, necessary simplifications during the processing phase and interpretational ambiguities. Further, the underlying data are usually distributed unevenly, e.g. clustering in regions with economically interesting reserves, while being very sparse elsewhere, so that the 3D modelling involves interpolation across wide distances.

This uncertainty characterizing the 3D models stands in stark contrast to the way in which the 3D modelling results are usually presented these days. The software packages that are used for 3D geological modelling, such as Skua-Gocad or Petrel, already provide visualization methods that are currently used to communicate the 3D models to the stakeholders or the public. Further 3D models are published on the world wide web, using the necessary web-technology to present these models in a browser. The visualization is usually done by rendering stratigraphic interfaces and faults as triangle- or quadrangle-meshes in 3D space and it pretends that the 3D subsurface is known exactly, sometimes giving the position of a mesh's vertices with a precision of up to a millimeter. In reality, however, we often do not know if a certain fault should be moved up or down a hundred meters, if it extends hundred meters more or less, or even if it actually exists at all or has a complete different shape. How can we estimate and handle the uncertainty and how do we express the magnitude and different types of uncertainty in our 3D models? Work package 4, "Uncertainty in Geomodels" which is part of the GeoERA project 3DGEO-EU, will work towards establishing the necessary workflows to provide a visualization of the 3D models, including their uncertainty.

This report, the second WP4 deliverable (D4.2), will give an overview of the different sources of uncertainty with emphasis on the methods and sources which seem to be most relevant for the construction of structural models. It will then show some practical examples how the propagation of this uncertainty into the build 3D models could be estimated using Monte Carlo simulation and/or Geostatistics.



TABLE OF CONTENTS

1	INTRODUCTION	5
2	SOURCES OF UNCERTAINTY.....	9
2.1	Overview.....	9
2.2	Uncertainty from borehole data.....	13
2.2.1	Uncertainty in the borehole trajectory.....	13
2.2.2	Uncertainty of tool position in the borehole.....	15
2.2.3	Uncertainty in the depth interpretation of formation boundaries ..	15
2.2.4	Uncertainty of inclination measurements in boreholes.....	16
2.2.5	Potential errors in a database with boring records.....	17
2.3	Uncertainty from seismic data	19
2.3.1	Overview of the sources of uncertainty in seismic data.....	20
2.3.2	Statistical estimation of horizon misties on 2D sections	21
2.3.3	Uncertainty in seismic interpretation.....	23
2.3.4	Defining a velocity model with uncertainty, using check-shots at wells	32
2.4	Uncertainty from acquisition to interpretation of the gravity data	34
2.4.1	Uncertainty related to gravimetric data	37
2.4.2	Uncertainty related to geological data	37
2.4.3	Uncertainty related to petrophysical data	38
2.4.4	Uncertainty related to gravity modelling (forward and inversion) ..	39
2.5	Uncertainty of field measurements.....	40
3	UNCERTAINTY AND 3D MODELLING.....	42
3.1	Overview.....	42
3.2	Estimating uncertainty for a regional 3D model in the Netherlands	44
3.3	Uncertainty for a voxel based model with high data density.....	47
3.4	Estimating uncertainty for a model with low data density in geologically complex regions.....	50
4	USE OF UNCERTAIN STRUCTURAL MODELS	55
5	REFERENCES.....	57



1 INTRODUCTION

When constructing 3D regional models of the subsurface, the geoscientist has to deal with a wide range of different types of uncertainty. As shown in Figure 1, the uncertainty should already be estimated and assessed during the acquisition and interpretation of the data which later form the basis of the 3D model. The location of markers for faults and horizons that are interpreted from borehole data is uncertain, especially when old logs from the archive have to be used, as the tools to determine the borehole path had, and still have, only a limited precision (see e.g. Wolf & Wardt, 1981). When seismic imaging is used, different sources of uncertainty are introduced in the different steps of the seismic processing sequence, especially during the time to depth conversion, as the velocity model can often only be estimated with a limited precision (for an overview, see e.g. Thore et al., 2002).

During the next step, namely the geometrical modelling phase during which the 3D geological model is built, the propagation of the uncertainty that comes from the input data must be assessed and its influence on the final model estimated. Sometimes there are insufficient data available for a large area and the modeller has to provide some kind of model-based interpretation in order to fill the void space in the 3D model. So the modellers have to make a decision on which conceptual models they should apply (e.g. the deformation style? flexure or fracture?) which introduces additional uncertainty, often called conceptual uncertainty. The approach commonly used to assess all these uncertainties in the resulting 3D model is the use of Monte Carlo Simulation (see, e.g., Wellmann & Regenauer-Lieb, 2012 or Schweizer et al., 2017). Different realizations of the 3D model are generated by first sampling into the input data. The depth of a borehole marker might, for example, be given as a Gaussian distribution function and for each realization the depth is randomly drawn from this function. Subsequently, a 3D model is generated for each set of randomly drawn data. These different models are then visualized or ideally could be summarized to be represented as one model which expresses the geology and its uncertainty (see, e.g. Wellmann & Regenauer-Lieb, 2012). When the resulting uncertain structural geological model is subsequently used for process simulation, it has to be propagated with attributes such as permeability, which also involves uncertainty. Many methods have been developed to treat this uncertainty, especially in the oil & gas and the mining industry to optimize exploitation and minimize risk (see e.g. Pyrcz & Deutsch, 2014).

The last, but nevertheless important, step in Figure 1 is the visualization. When the 3D models generated are presented to the public and the stakeholders, they should be made aware of these uncertainties in those models. Currently the representation of the geological models as triangle- or quadrangle-meshes often pretends that the position of geological structures is known to a precision of a centimetre. It is one of the primary targets of this work package to find a good visualization which shows the uncertainty in 3D geological subsurface models and where this uncertainty is coming from. The visualization should be easy to understand and intuitive and might vary for different types of viewers, e.g. for experts and novices.

The aim of the work package “Uncertainty in Geomodels” is to structure the whole discussion on uncertainty in our 3D geological models and its quantification and visualization from the viewpoint of geological surveys. What is already there and where are the gaps? The work package will provide a knowledge base to assist in the future use of the visualization methods



already established in geosciences and also establish the basis for future cooperation with other research disciplines, such as computer graphics, to fill the gaps identified.

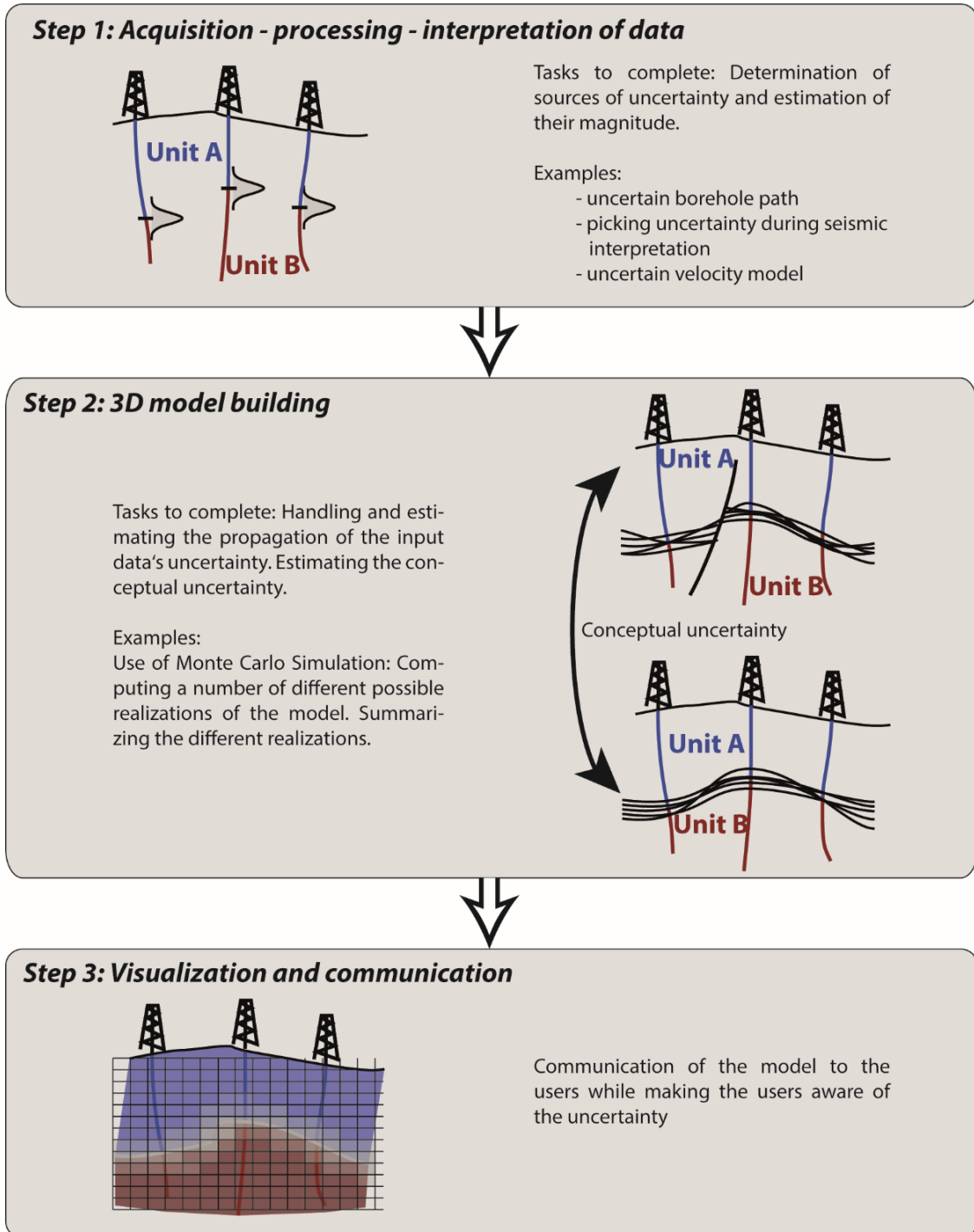


Figure 1: The different general steps to build and display a 3D geological model where the uncertainty has to be assessed.



In order to achieve this, the whole work package is structured in terms of four different tasks (see Figure 2). During the first half of the project, the aim of the first two tasks will be to establish and document the methods and concepts required. Task 1 captures the state of the art in uncertainty visualization (options for step 3 in Figure 1) and in this manner also provides information about which type of data we need to compute in order to be able to display the uncertainty in our models. It thus sheds light on where we might go and what we will need for it. Task 2 will discuss the different sources of uncertainty and the methods to propagate this uncertainty through the 3D modelling process (steps 1 and 2 in Figure 1). Task 3 and 4 in the second half of the project will apply the methods described to test different visualization options, using data sets from the pilot areas of the 3DGEO-EU project.

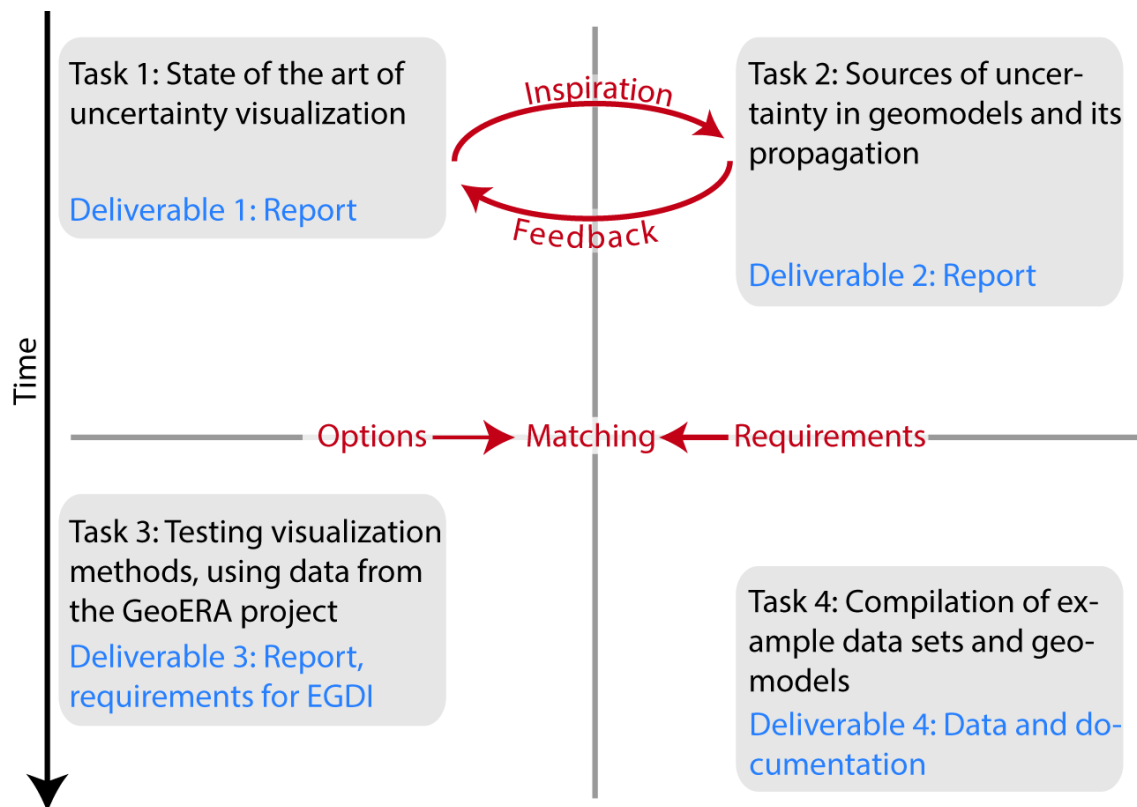


Figure 2: General structure of the 3DGEO-EU work package “Uncertainty in Geomodels”.

The overall outcome of the project will be a structured and documented overview of what is already available for the treatment and visualization of uncertainty and will thus act as a point of transfer for the necessary knowledge and skills from computer sciences to geosciences. Further it will try to suggest some best practices and workflows for how the visualization of uncertainty could be incorporated into the current standard workflows for 3D geological modelling. Finally the work package will identify what still needs to be developed and provide the necessary means, gap identification and corresponding example data sets, to give potential



outside partners, such as computer graphics groups at universities, the motivation to do research towards developing the methods lacking.

This report is the deliverable of Task 2. It will outline the different sources of uncertainty that have been identified by the project members and try to describe some quantitative estimate in Chapter 2. Different methods to estimate how this uncertainty, coming from the primary sources, is propagated through the 3D modelling process and how it affects the final model. In a later stage of this work package, the visualization requirements emerging from this report will be matched to the available methods described in the report on the state of the art in uncertainty visualization (Deliverable 4.1) to identify gaps and optional future areas of research. This match will be done based on the classification / typology of data and their specific uncertainty. As a result, two sets of requirements will be identified. The first set consists of data types and uncertainty types for which visualization methods exist already and which could be implemented as part of a 3D viewer of the information platform (EGDI). The second set consists of data and uncertainty types for which no visualization method seems to have been established so far. Here further research will be required. The user requirements, gaps and research requirements found will be documented in Deliverable D4.3. Further documented example data sets will be provided (Deliverable 4.4).



2 SOURCES OF UNCERTAINTY

2.1 Overview

In general we can distinguish two types of uncertainty, aleatoric and epistemic uncertainties. Aleatoric uncertainties are induced by randomness, such as tossing a die, and are often associated with repeatable experiments. Epistemic uncertainty is due to imperfect knowledge about something that is not in itself random and is, in principle, knowable (O'Hagan et al., 2006). It is typically associated with unrepeatable processes and thus cannot be determined by experiments using statistics.

Due to these different kinds of uncertainty, it is also worthwhile to keep the discussion of Frodeman (1995) on geology as an interpretive and historical science in mind. Often it is assumed that science should be certain, precise and predictive, and that scientific knowledge can be analytically derived. This holds for physics and methodically closely related subjects, such as geophysics and engineering. Other scientific subjects are judged in terms of how well they meet these standards. However, Frodeman (1995) points out that the lack of experimental control, the great spans of time required for geological processes to take place and the incompleteness of data make direct observations difficult, if not impossible. Frodeman (1995) thus suggests that geology should instead be seen as an interpretive (hermeneutic) science. The comprehension of a certain problem is built up in an iterative fashion (the hermeneutic cycle) as we revise our conception of the whole (e.g. a certain region) based on the new meaning suggested by the parts (e.g. recently examined outcrops), and our understanding of the parts through our new understanding of the whole.

In practical terms, this means that geoscientific investigations lead to a wide range of uncertainties that are aleatoric and/or epistemic. Geologists often make use of geophysical methods to gain information about the subsurface. These methods follow the rules of physics and mostly deliver data with aleatoric uncertainties, which are, for example due to the precision of the measurement instruments, such as logs that are lowered into a borehole. Further, some information can be directly gained from outcrops but imprecisions arise due to the variability and imperfections of nature and the exactness with which geologists can work in the field. A structural measurement with a geological compass, for example, can only be read with a limited precision by geologists, and often varies depending on which location of bedding or cleavage plane in an outcrop has been chosen, due to the bumpiness and roughness of the rock. For this reason, it is common practice to measure the data at several locations, even in the same outcrop, and then to calculate the mean. These aleatoric uncertainties are often easy to assess, for example by using statistics in the case of field measurements or by obtaining the precision of the instrument from the manual of the manufacturer.

However, the data only provide information on the physical properties for the exact location where they are measured and the interpretation of the acquired data and the extrapolation away from the measurement locations often involves ambiguities and non-uniqueness. Thus, interpretation relies heavily on the knowledge, ability and experience of the interpreter and so leads to epistemic uncertainty that is much harder to control and to assess. This becomes particularly apparent when data are sparse and discontinuous, and so can only be interpreted jointly in a limited way. To give an example: imagine a small 5x5 km area for which a 3D seismic



with good quality and well visible reflectors together with a couple of boreholes is available. This area can clearly be modeled with a much higher confidence than a 25x25 km large region for which only a few 2D seismic sections and a borehole is available that is even not on one of the sections - at least when the general background data, such as structural complexity, is comparable. It seems likely that this epistemic uncertainty effects geological services and their workflows more than industry. Most projects in industry have, due to the economic interest in them, relatively well-funded data acquisition and deal with relatively small-scale models, such as reservoirs. In contrast, Geological Survey Organizations often build large regional models, such as the TUNB model of the North German Basin (TUNB, 2021), the GeoMol models of the Molasse Foreland Basins of the Alps (GeoMol, 2021) or the TNO models of the deep and shallow Dutch geology (TNO 2021). Within these areas, they might have some regions with good data coverage, but between these regions, large spaces appear often where data coverage is small. This becomes especially true for the deeper underground.

The epistemic uncertainty that is based on the different possible interpretations and the way of reasoning is much harder to assess, because it requires that people would need to quantify with what probability they follow a certain line of reasoning. The experts would need to make a choice regarding which hypothesis is most likely and estimate its probability in comparison to the other hypotheses. Baddeley et al. (2004) and Tversky and Kahnemann (1974) explain that this judgement of probability is prone to make some common mistakes, due to cognitive limitations in the processing ability of the human mind, which lead to biases in the estimation. Based on (a) Baddeley et al. (2004), (b) Tversky and Kahneman (1974) and (c) Bond (2015) the following hierarchy can be sketched to give some examples:

○ **Individual bias:**

- **Motivational bias:** This reflects the interests and circumstances of individual experts. They might want to appear knowledgeable because their job depends on the decision or they might be influenced, or even forced, by their management, to favour a certain solution. This bias is usually under rational control and thus can be manipulated and controlled.
- **Cognitive bias:** This reflects the incorrect processing of information and is not under conscious control. The reason for this is that experts often rely on heuristics or rules of thumb that are based on their experiences and which they use to make relatively quick decisions in uncertain situations:
 - **Availability (a, b, c):** The probability is assessed by the ease with which occurrences of an event is brought to mind. This might, for example, be influenced by the most recent and prominent or most interesting field or interpretation examples an interpreter might have had experienced.
 - **Anchoring and adjustment (a, b, c):** Often an initial value for the probability is estimated or has already been given – known as the ‘anchor’ - and then needs to be adjusted due to new or additional information. This often leads to results which have a bias towards the initial value.
 - **Control (b):** People have the tendency to act as though they can influence the situation, even if they cannot. So, even if the process is completely random, people prefer to make a choice.



- **Representativeness (a, b):** Probabilities are evaluated by the degree to which an object A resembles, for example, a class-template (e.g. a stereotype) B. If A is similar to B, the probability that it belongs to B is assumed to be high, otherwise it is considered to be low. This involves several pitfalls:
 - The prior probability is often neglected (base-rate neglect) - what is the probability that A belongs to class B without any comparison?
 - When a series of trials all have the same outcome, people expect that the probability of the other outcomes rises. In reality it is always the same (gambler's fallacy).
 - When events are compounded, people tend to overestimate events which are compounded using the logical 'and' and to underestimate events that are compounded using the logical 'or'.
- **Confirmation (c):** Hypotheses are favoured that confirm the interpreter's own beliefs.
- **Optimistic (c):** Overestimation of the likelihood of positive events, as the interpreter wants things to come out for the best.
- **Group bias:**
 - **Paradigm anchoring (a):** Often the beliefs of experts are anchored to the existing dominant paradigm and thoughts are forced to stay within certain boundaries.
 - **Herding (a):** Experts might have incentives to follow the opinion of other experts, for example when they assume that their estimations are based on better information. The opinion of the other experts is then treated as being part of their own prior information.

However, when looking at possible explanations for some of the cognitive biases given above (see, e.g., Kahneman, 2011), these often have their roots in insufficient control of our automatic and quick way of thinking that is not under voluntary control and helps us, for example, to recognize if a person is in good mood or aggressive (System I in Kahneman, 2011). This is often used instead of a more effortful and deliberate way of thinking that also might include complex computations (System II in Kahneman, 2011). Most of the experiments that are given to showcase these effects require quick decisions on fairly easy tasks. However, creating a reservoir model, for example, from a couple of seismic sections and additional borehole information, usually takes a long time and involves moving from one section to the next and back and forth, possibly following more the way of reasoning described in Frodeman (1995). So the question remains as to whether these two situations can be compared.

When several experts are involved, it might also be worth looking at the group dynamics and being aware of the influences the individuals might have on each other. Kahneman et al. (2021) suggest, for example, that it is important to let the individuals in a group first work out and write down their judgements of different possible interpretations independently before discussing this as a group. Otherwise there is the risk that the expert group is subject to informal cascades, where the view of the first expert who explains his opinion influences the views of the others. In order to elicit the information on probabilities from the interpreters, it is therefore necessary to use appropriate methods (see, e.g. Curtis & Wood, 2004, or O'Hagan et al., 2006). Further Polson & Curtis (2010) made experiments and pictured how experts might change their view during a group elicitation experiment. This experiment also shows that expert's views can have a relatively wide range when the data are ambiguous and imprecise, and that therefore results from an expert should not be seen as unique.



The following sub-sections outline the sources of uncertainty which the different project partners have identified during the 3DGEO-EU project and give an overview of the available literature. During the starting phase of the work package a questionnaire was used to assess which data types and acquisition methods are mainly used as input data for the construction of 3D geological models (see Figure 3). As can be seen, there is a strong emphasis on borehole data and seismic data, followed by the current maps, which are an interpretational product itself for which the uncertainty has usually not been assessed in the past. Sometimes the field record is used, and sometimes potential field methods are used to constrain the model further. The use of gravimetric methods, even if not used very frequently by most of the project partners, is an important part of one of the work packages in the 3DGEO-EU project and a more detailed discussion of the overall workflow applied and the corresponding uncertainty is given in Deliverable 6.4 (Pueyo et al., 2021).

Further the focus is placed on those sources over which the partners have influence during their work. The seismic data that are used, for example, are mostly acquired by external companies and have been preprocessed, stacked and migrated by these companies. Sometimes the uncertainty is given in the accompanying report. In such cases, the project participants do not have the necessary experience to elaborate further and they potentially do not have the necessary data and software to assess the uncertainty. However, in these cases this report will try to point to relevant literature that can be used as starting point.

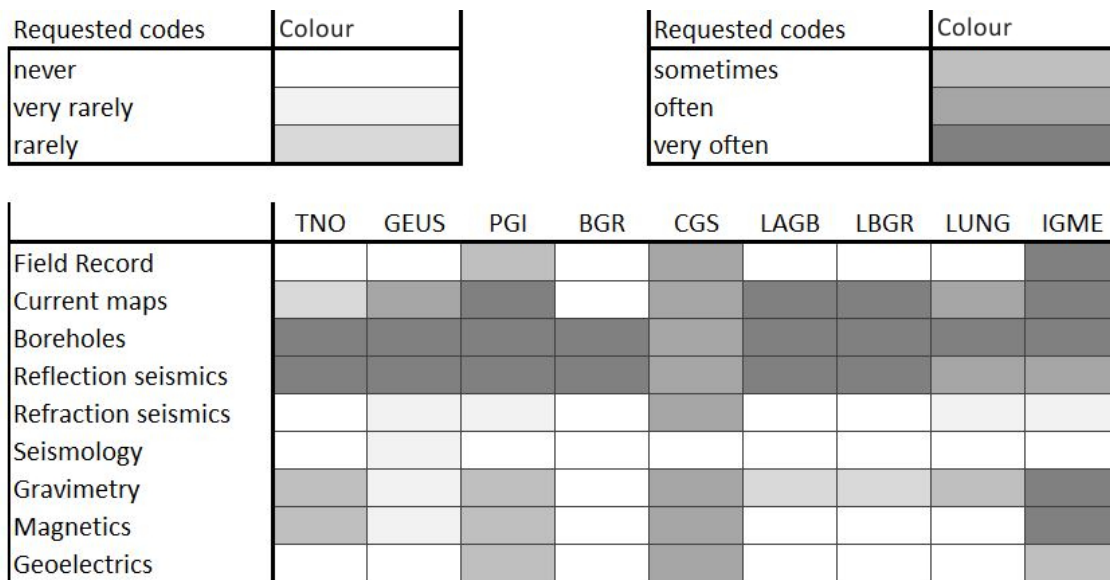


Figure 3: Frequency of usage of different data types by the project partners involved in 3DGEO-EU Work Package 4 (Uncertainty in Geo-Models) for structural modelling of the geological subsurface. However, the figure reflects neither the overall usage of data in their organization nor the usage of data for other purposes.



Overall the assessment during the starting phase has shown that the assessment of the uncertainty of the generated 3D models is still in its infancy and has only been done recently by very few of the project partners.

2.2 Uncertainty from borehole data

Overall, there are several factors that influence the precision of a borehole geophysical measurement. The following section focuses on factors which affect the precision and accuracy of depth and positional information from borehole geophysical measurements:

- Uncertainty of the borehole trajectory
- Uncertainty of the tool position in the borehole
- Uncertainty in depth interpretation of formation boundaries.

However these different factors are not interdependent. They each have to be analyzed regarding their magnitude, and the resulting uncertainties have to be combined.

2.2.1 *Uncertainty in the borehole trajectory*

The borehole path is usually calculated from the measured depth (MD) along the borehole, the inclination (deviation from the vertical borehole path in degree) and the azimuth of this deviation in degree (angle to the north axis). For most tools (not for Gyro tools), conditions for a correct deviation measurement are a complete stop and a stable position of the tool. Consequently, deviation surveys are performed at certain intervals/steps (nowadays every 3-4m, in former times 25-100m). It should be kept in mind that these step lengths are also uncertain, as there is a depth measurement error, for example due to friction of the tool in the hole, which was estimated by an operator to be between $MD \cdot 0.2 \cdot 10^{-3}$ and $MD \cdot 1.5 \cdot 10^{-3}$ (Wolff & Wardt (1981)). The borehole trajectory is then calculated as a succession of individual straight segments from these measurements. Changes in borehole trajectory in between the stations will not be recorded and lead to an additional uncertainty. The effect will increase for large station intervals.

The uncertainty in these individual measurements of azimuth and inclination depends on the type of tool that has been used.

- Single- and multishot devices (used in open holes, not ore-bearing formations): These tools use a gimbal-mounted magnetic compass for the registration of the azimuth and a pendulum for measurement of the inclination of the borehole. For early tools, the compass readings and the position of the pendulum are photographed in the borehole and recorded on a film (Fricke & Schön, 1999). The magnetic compass is covered with a glass panel with a compass rose with a 5-10° scale division for the azimuth reading and a 1-2° scaling for the inclination reading (Lehnert & Rothe, 1962). For analogue compasses, azimuth readings in between the tick marks are possible to a precision of about $\pm 2^\circ$ (Inglis, 1987) and inclination readings with an accuracy of about 0.5° . Digital compass tools with a higher precision are able to measure the azimuth as precisely as about $\pm 1^\circ$ and the inclination by about 0.1° (Wolff & Wardt, 1981). However, inaccuracy of single- and multishot devices can be higher due to the daily fluctuation of the declination of the earth's magnetic field (to the order of



0.1°), magnetic storms (several degrees), the presence of ore (several degrees) or bad borehole condition affecting the reading on the glass panel. Additional uncertainty on the readings is introduced by the magnetization of the drill collar, which influences the deflection of the magnetic compass needle. This effect depends on the current direction of the borehole and is shown to be higher for highly inclined boreholes and for east-west trending boreholes. Wolff & Wardt (1981) calculate an example where they show that this error can be up to several degrees.

- Gyro instrument (used in open and cased holes, as well as in ore-bearing formations): The installed gyro instrument can freely move about any axis. As is usually the case for normal gyros, throughout the survey a drift (affecting only the azimuth reading) is observed. Compensation is performed by assessing the closure based on the linkage of the up- and down-run. The usage of “north-seeking” gyro (rate gyro) can reduce (not entirely eliminate) the drift effect. In nearly vertical boreholes, processed data of a measurement with a well calibrated gyro and a precisely determined orientation at the surface, allows an accuracy of the azimuth measurement to less than $\pm 1^\circ$ and a quite precise reading of the inclination about 0.03° (Wolff & Wardt, 1981). Internal experiments at the LAGB (Landesamt für Geologie und Bergwesen - the Geological Service of Saxony-Anhalt), including repeated measurements and several processed gyro surveys, indicate that the achieved precision of the azimuth reading in a borehole that is about 30° inclined decreases to 2° , even if the technical precision of the instrument that is given by the manufacturer is higher.
- Strain gauge tools (used in cased holes, as well as in ore-bearing formations): These tools are used in the drill string and are equipped with accelerometers to measure the inclination. The measurement of the azimuth is performed by means of small spring-loaded wheels, which run at the inner side of the rods. A bending of the drill string results in changes in the length of the springs, which are transformed to changes at the strain gauges and converted to a difference in azimuth to the previous measurement. In contrast to the accuracy quoted by the manufacturers (inclination about 0.2° for total borehole length, azimuth about 0.01° per reading), repeated measurements done by LAGB in the field in inclined boreholes revealed an inclination accuracy of about 0.5° and an azimuth accuracy of about 0.02° per reading.
- All tools – poor centralization: During a measurement, the compression of the centralizers of the tool may differ due to the rugged borehole wall or twist of the wireline. As a consequence, the tool will slightly rotate and/or misalign from the vertical axis. This effect is smaller for tools running inside the casing and/or if it is rotated in between the measurements (strain gauge tools). Consequences of bad centralization become even worse in inclined boreholes and can be to the order of 1° (Wolff & Wardt, 1981).

Some of the measurement errors are dependent on the region in which they are measured and it can be assumed that the precision of the instruments and the overall technology has improved over time. Wolff & Wardt (1981) give typical values for these measuring errors in the North Sea based on the state of the art at that time and discuss how these errors could be aggregated along the boreholes and be presented.

However, even if nothing is known regarding the instrumentation and measurement procedures, for example in old reports, some minimum uncertainty can be estimated from the given numbers, as it is common practice to give the readings with the precision with which they



can be done. Looking at some reports, the inclination was often given with one decimal place which shows that the uncertainty is at least 0.05° . Further the azimuth was sometimes given in 5 degree steps which indicates that the uncertainty is at least ± 2.5 degrees. To gain an insight into the magnitude of the errors introduced by such an uncertainty, we have used an approximately 4000 m long borehole in Skua-Gocad and assumed the extremum, a constant drift of the instrument with $+0.05 / -0.05$ degree in inclination and $+2.5 / -2.5$ degree in azimuth. In the first case, the spread of the resulting borehole paths at the bottom was of the magnitude of 6m and in the second case of the magnitude of 30m.

2.2.2 Uncertainty of tool position in the borehole

Besides the inaccuracies in determining the trajectory of the borehole in the subsurface, additional uncertainty is caused by the missing control on the positioning of the tool inside the borehole (see Figure 4 for an example). As described in section 2.2.1, a tumbling of the tool results on the one hand in inaccurate deviation measurements. On the other hand, the interpretation of orientation measurements will be affected.

Uncertainties may exist as well about the depth of a specific measurement in the borehole (affecting all borehole geophysical measurements). Main reasons for this are local friction and the sticking of the wireline at the borehole wall, lengthening of the wireline due to high temperatures and its own weight as well as differences in the twist of the wireline. Without a correction for these effects, resulting depth uncertainties are of the order of $MD \cdot 0.2 \cdot 10^{-3}$ and $MD \cdot 1.5 \cdot 10^{-3}$ (MD = measured depth [m]) (Wolff & Wardt, 1981). These inaccuracies can be reduced by the use of a casing collar log (magnetic or electromagnetic tool) combined with a gamma ray sensor. The casing collars will be located as precisely as $MD \cdot 0.1 \cdot 10^{-3}$ and can be linked to the other geophysical measurements by the gamma ray log.

2.2.3 Uncertainty in the depth interpretation of formation boundaries

Often the positions of the stratigraphic interfaces along the boreholes (borehole markers) and other important geological features are taken from bore logs, databases or drilling reports. In these cases it would be important to examine how the location of the markers (interfaces) has been determined and to estimate or assess the corresponding uncertainty.

- The position of the stratigraphic interfaces could be derived from the lithology which is often interpreted by the well-site geologist and the mud loggers from drilling cuttings or from borehole interpretations. However, there are several uncertainties involved when defining the depth of the stratigraphic interface as the result of observations in the drilling cuttings. The drilling cuttings often need several hours to be transported from the bottom of the well to the top with the drilling mud. Experiments by Naganawa et al. (2018) show that they are dispersed during the transport, resulting in a log-normal distributed arrival that has increasing variance (smearing) in highly deviated or horizontal boreholes. Further, the cross section (volume) of the borehole and so the velocity of the drilling mud is not known exactly and the cuttings are usually collected as composite samples for an interval that could be, e.g. according to Whittaker & Morton-Thompson (1992), 10 feet. When interpreting a stratigraphic interface from a certain set of cuttings, two different types of uncertainties have to be considered. Firstly the uncertainty of the depth in the borehole from where the



set of cuttings is coming, and secondly the uncertainty that the deduction of having found the interface is correct at all.

- The position of the stratigraphic interfaces can be directly derived from well logs. To obtain accurate depth information, it is necessary to account for the tool's reference point (depth position of the sensor inside the tool or if several sensors are necessary for a reading, the midpoint of the arrangement is required). Not accounting for these differences will lead to uncertainties to the order of up to 1m. Nowadays, most borehole geophysical tools are equipped with a gamma ray sensor. During processing the depth shifts observed between the gamma ray logs of the different tools also allow a correction for the differences in their reference point. The resultant accuracy of the depth information is about 0.2m.

In practice (and as a rule of thumb), stratigraphic boundaries are usually assigned at the turning point of the log's curve. However, an exact determination of the interface (slightly off the turning point) varies for the different borehole geophysical measurements and requires additional factors to be taken into account, such as the setting of the tool, the logging speed, the thickness of the layers, the characteristics of the upper/lower formation, the signal-to-noise ratio, resolution of the data and in some cases the time constant of the measurement. Finally, the characteristic of the interface itself (distinct or gradual) has an influence on its exact determination (e.g. Reading & Gallagher, 2013). If some of the acquisition parameters are unknown or not accounted for, uncertainties in determining the correct depth of the interface are for most scenarios in the order of 0.2-1.5m.

Measurements recorded with an analogue system (such as is the case for most surveys in the former GDR) carry an additional uncertainty. After recording and as preparation for the subsequent interpretation, all curves were manually redrawn and merged on large sheets of paper. As usual, such a transfer is problematic and observed depth errors have magnitude of up to 2m.

- Finally the position of the geological features could be derived from cores, which should be the most precise source of information. However, in highly fractured or weathered zones, a quite considerable amount of material might already have been washed out by the drilling fluid. The same might be true for sections of anhydrite or salt, which might dissolve when coming in contact with the drilling fluid. Further, careful tracking of the orientation of the core is required, even when experiencing problems in retrieving the rods (with the core inside) as well as during the boxing up of the core.

2.2.4 Uncertainty of inclination measurements in boreholes

As will be discussed further below, some of the 3D modelling approaches can not only take the depth and position of a borehole marker as a constraining input but also its orientation (see e.g. Calcagno et al., 2008). Stigsson and Munier (2013) discuss the uncertainty of orientation measurements for fractures, done on the basis of borehole image data, and how these are affected by the uncertainty of the borehole orientation. Presentation and discussion is done on the basis of a Stereonet (Equal Area Projection).

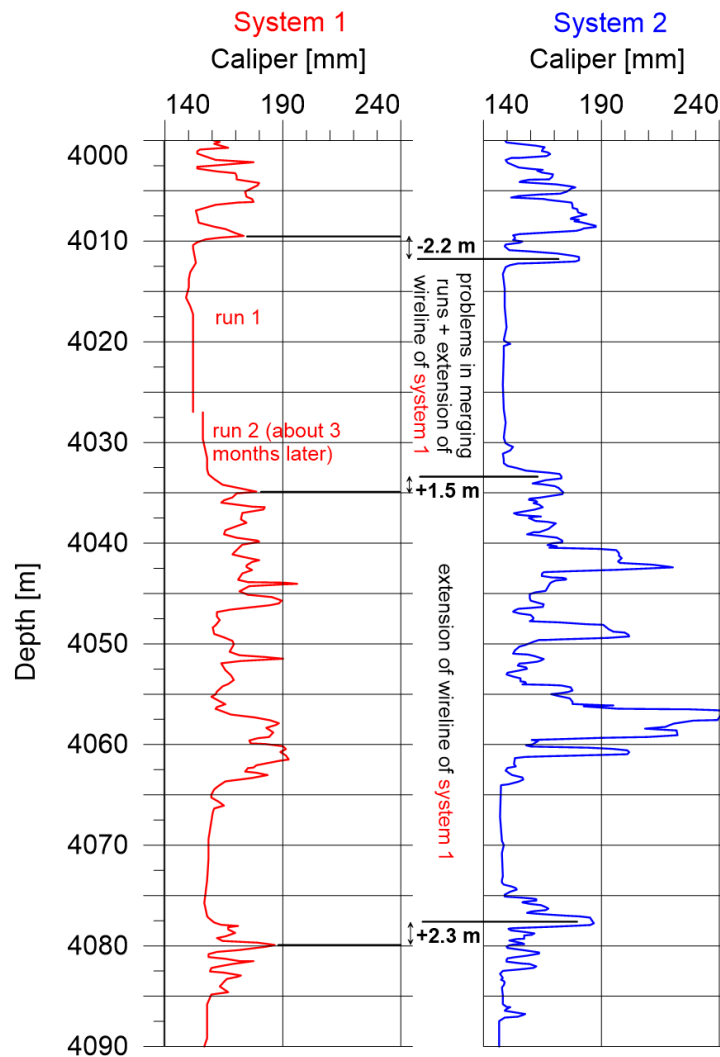


Figure 4: Example from a borehole in Saxony-Anhalt (drilled in the 1980s), demonstrating two factors influencing the accuracy of depth information from borehole logs. 1.: Former merging of the different runs with system 1 caused problems in depth correlation and amplitude. 2.: The caliper measurement was repeated with a second system, consisting of different tool, wireline and recording unit. Comparison between the surveys reveals an extension of the wireline of system 1 (measured temperature in 4000 m depth was 149°C).

2.2.5 Potential errors in a database with boring records

Often and especially when large datasets are used, the measured depths of borehole markers are directly taken from databases. Thus the original borehole information, which in general stems from printed reports collected over decades, became digitized, reinterpreted and sometimes converted into modern stratigraphic encryptions. Afterwards interpreted stratigraphic or petrographic boundaries were converted into the model's stratigraphy using mapping lists. Due to the large amount of borehole information and its heterogeneity, the



question arises as to how reliable these data are and which kinds of discrepancies probably lead to uncertainties for the modelling process. Although this cannot be assessed in general, the following discussion will provide an idea for uncertainty estimates.

- **Typing errors in stratigraphic/petrographic encryptions:** Typing errors can occur during each digitalization step, when borehole data are entered into a borehole database (horizontal and vertical position, measured depth, stratigraphic encryptions, etc.). Due to the fact that modern database systems are commonly supported by dictionaries and thus propose legitimate encryptions for stratigraphy, petrography and genesis, typing errors in encryptions can be reduced to a certain degree. Nevertheless, the use of dictionaries does not prevent the digitizer from deciding which encryption is correct for the region where the borehole was drilled (e.g. International Chronostratigraphic Chart; Cohen et al., 2013; vs. Stratigraphische Tabelle von Deutschland; German Stratigraphic Commission, 2016; vs. Symbolschlüssel Geologie; Landesamt für Bergbau, Energie und Geologie; 2015). Thus, even if spelling and grammar of encryptions equates to dictionaries, we cannot fully assume that the encryption corresponds to the regional geology.
- **Typing errors in coordinates and depths:** Typing errors in the position of markers or coordinates of complete boreholes can arise during each step of digitalization and are difficult to detect. Typically, they arise when single digits of coordinates or depths were incorrectly typed. Although the appearance of typing errors is relatively low (< 2 % of typed boreholes/markers), single errors might heavily affect the precision of information. If several hundreds of boreholes are used for 3D modelling, we have to suspect that at least some of them are represented at an incorrect position. Furthermore, we have to keep in mind that approximately 30 % of boreholes contain at least one incorrect marker position. Although for deep boreholes (several kilometers deep) with several hundreds of markers that error (< 1 %) might appear insignificant, the bulk of the errors (approx. 73 %) show a deviation larger than 10 meters in depth (Figure 5) and thus is not insignificant.
- **Stratigraphic interpretation/encryption stored in borehole databases:** Stratigraphic interpretations and encryptions in borehole databases depend heavily on the interpreter's choice during rock classification, stratification and well-log evaluation. That is why borehole databases typically contain a strongly heterogeneous inventory. Interpretations and descriptions are based on the stratigraphic knowledge and encryption at the time when the borehole was interpreted. Typically it is performed for one single borehole. Afterwards, i.e. after further analysis (e.g. micro paleontological, petrophysical or geochemical analysis) or regional correlations, boreholes often become re-stratified and re-interpreted, which leads to various geologic profiles for single boreholes. They contain descriptions and encryptions based on schemes current at that time. These schemes may have changed since the borehole was originally interpreted (Franz et al., 2018; Hiss et al., 2018; Mönning et al., 2018 and references therein) or vary across regional, geological, prospective or political borders. Thus borehole database information can be strongly heterogeneous, vary over small distances and contain inconsistent data, if no standardized schemes and interpretations were used.
- **Conversion of borehole information into model stratigraphy:** Due to the large number of boreholes (some hundreds of thousands) stored in databases, a unified stratification and encryption is most often not warranted. Hence, converting stored information into model



stratigraphy is not a straightforward process and has to be considered with care. Encryptions vary from one borehole to another with respect to their level of detail. Even for smaller models (i.e. some tens of square kilometres) containing some hundreds of boreholes, the number of different encryptions can easily exceed several thousands. These encryptions need to be systematically generalized and summarized with respect to the model resolution and detail.

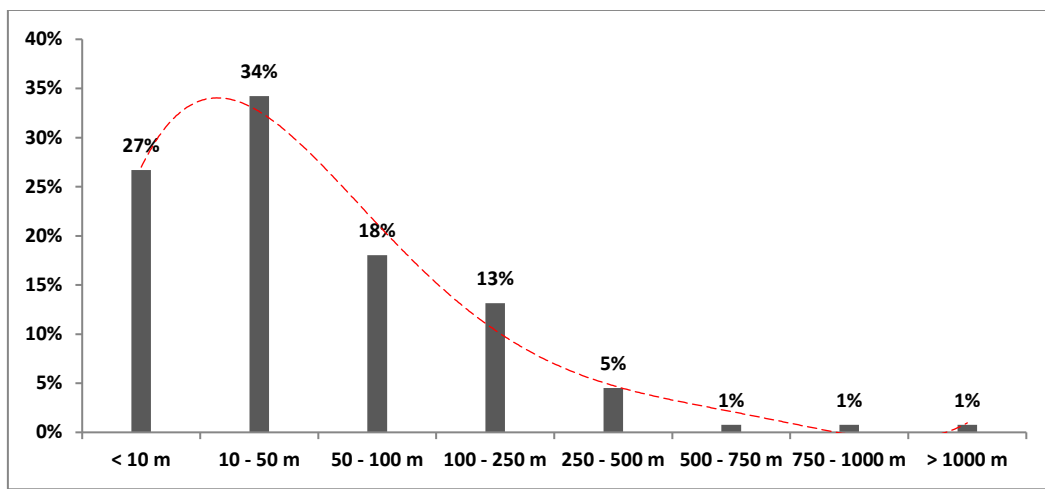


Figure 5: Diagram illustrating the deviation in depths due to typing errors. For analysis 835 deep wells (drilled by the petroleum industry) from the borehole database of Saxony-Anhalt were used. A running number generated during along-depth digitalization enabled us to determine the range of uncertainty. 274 boreholes (32.8 %) contain at least one typing error (0.4 % if assuming approx. 250 markers per well).

2.3 Uncertainty from seismic data

As can be seen from Figure 3 on page 12, reflection seismics is very often used by the different project partners and the assessment of its uncertainty is for this reason important to estimate the uncertainty in the 3D models generated. However, the different project partners of the GeoERA project 3DGEO-EU mainly work with data that where processed by third parties (e.g. by the oil & gas industry), and for this reason mostly have no option to do an analytical error estimation. However, instead of trying to do such an error estimation descriptive statistics could be used at several phases of the project to get an insight into the uncertainty that is due to the different processing problems described above.

In the following a short introduction on the different sources of uncertainty will be given, pointing to some relevant literature. Then different options will be discussed to assess the uncertainty experimental, using statistics, and finally we will give some examples on the uncertainty that arises due to interpretational issues.



2.3.1 Overview of the sources of uncertainty in seismic data

Thore et al. (2002) discuss the uncertainty in the final structural model due to the different seismic processing steps (acquisition, preprocessing, stacking, migration, interpretation and time-to-depth conversion). According to them, the errors and imprecisions during the acquisition, preprocessing and stacking phase will mainly lead to a fuzzy or possibly worse to an absent image but will not dislocate the reflectors, and thus will not increase the uncertainty in terms of positioning features of the structural model. In contrast to this, the latter three phases have a major impact on the structural uncertainty.

For the migration and the time-to-depth conversion, this is due to the uncertainty in the velocity model and most likely will shift horizons, faults and other structural elements, such as salt structures, while keeping the overall topology of the structural framework. Parkes & Hatton (1987) describe how ray-theoretical modelling together with perturbation of the velocity field (Monte Carlo simulation) can be used to study the influence of errors in the velocity model on depth- and time-migration on a 2D section. Loveridge et al. (1987) extend this approach to the 3D case but are limited to studying the effects on time-migration. While the influence of uncertainty in the velocity model on the generated depth-migrated image is high, the influence on a time-migrated image is fairly small. The migration error is greatest where dip is steepest and is proportional to the displacement and hence to the magnitude of the dip. Overall Loveridge et al. (1987) conclude for time-migration with an uncertain velocity field, that the migration error is small in comparison to migration displacement.

During the interpretation phase multiple sources for uncertainty exist, such as the precision with which the different reflectors are picked. Further, an additional uncertainty is added during the interpretation phase that is due to the quality (contrast, continuity) of the seismic image and the fact that it is often unclear which geological concepts should be applied (conceptual uncertainty). This uncertainty affects not only the position of the geological structures but the topology of the structural model. The conceptual uncertainty can be reduced when borehole information is available and information on the geotectonic history and deformation style can be used.

Finally the time to depth conversion creates uncertainty about the final position of the horizons and geological structures. Thore et al (2002) estimates that this uncertainty often contributes up to, or more, than 50% to the overall uncertainty in rock-volume estimation. This is mainly due to the large uncertainty in the velocity model.

In the following subsections we will first show how the overall uncertainty inherent in the depth of reflectors in 2D seismics could be estimated statistically and independently of its physical sources when a sufficiently large number of crossing 2D sections are available. This could be seen as a useful approach to estimate statistically the lower bound for the uncertainty of the depth of the reflectors in the time-domain, which is due to the first four processing steps (acquisition, preprocessing, stacking and migration). The approach could be used when no systematic treatment of uncertainty for these steps is available. We will then discuss in a little more detail which interpretational problems with 2D seismic could arise, using a 2D seismic section from the German North Sea sector. Finally we will show how a velocity model that incorporates the uncertainty could be constructed, using an example from the Netherlands. This



uncertain velocity model could then be used to assess the uncertainty in the time to depth conversion (see section on uncertainty and 3D modelling below).

2.3.2 Statistical estimation of horizon misties on 2D sections

Sometimes, for example in the North Sea, a large number of 2D seismic sections are available that are not all parallel to each other and so define a number of intersections. Reflectors that are visible on both crossing sections should match at the intersection but often do not. This is due to the different uncertainties mentioned above. The seismic sections might have been processed in a different way and with different quality, and further the migration is only done on the section while clearly migration components that point out of the section should be involved. Evaluating the misties at all intersections could potentially give an overview of how large the uncertainty is without necessarily having to understand where it is coming from. In order to illustrate this, we have estimated the misties for two horizons on a large set of crossing 2D seismic sections in the German North Sea which are currently used for constructing a 3D model of the deeper subsurface within the project TUNB (TUNB, 2020). Figure 6 shows the crossing points located on a map and coloured according to the magnitude of the misties. On a few occasions (see below) they can become very large and so the colour scale has been clipped at 100ms.

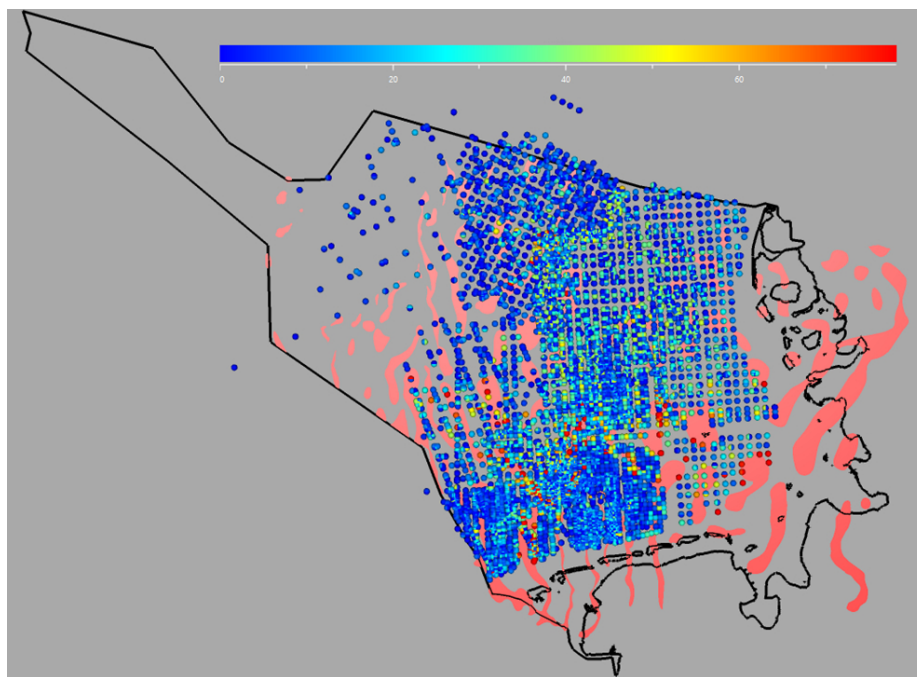


Figure 6: Uncorrected misties for the T1 (base Tertiary) reflector of crossing 2D seismic sections in the German North Sea sector. Colours indicate the magnitude of the mistie and are cut at 100ms, so that misties above 100ms are coloured all in red. Black lines indicate the borders of the German Sector and the German coastline with the North Frisian and East Frisian isles. Pink areas in the background indicate the approximate extend of the major salt structures (salt diapirs, salt domes and salt walls).



As can be seen from the histograms in Figure 7, only a small fraction of the misties for the KR2 and T1 reflectors are larger than 50ms. As it is not known which of the two sections that are crossing is actually wrong, only the absolute value of each mistie is taken which leads to this asymmetric histogram shape.

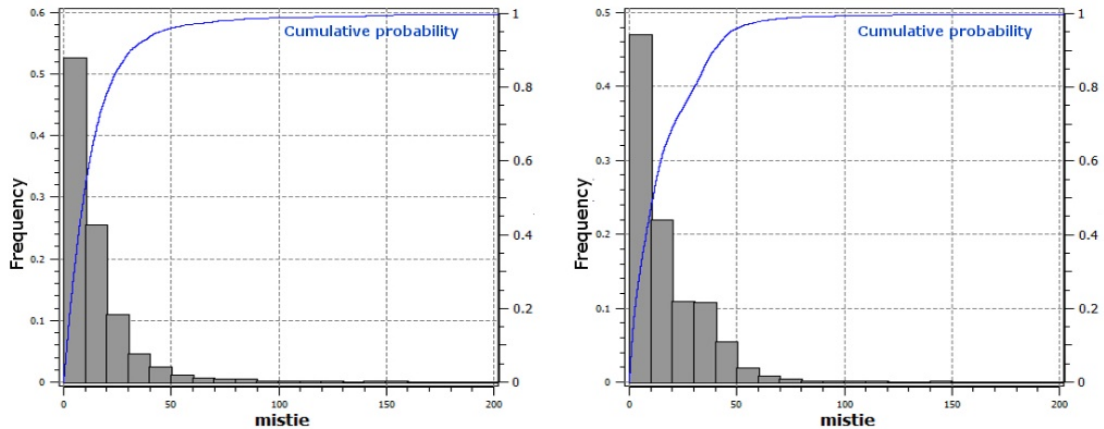


Figure 7: Histograms for the misties of the Kr2 (left) and T1 (right) reflectors.

While most misties for both reflectors are below 50ms, some may have a much higher magnitude of up to and seldom even more than 200ms. It has been suggested that these high misties might be caused by salt structures in the subsurface. In order to test this hypothesis, we have calculated the map distance to the salt structures (pink areas in Figure 6) and generated cross-plots of map distance against mistie. As can be seen from the cross plots all points that exhibit a high magnitude for the mistie, for example are higher than 75ms, are near to salt structures (closer than 5000m).

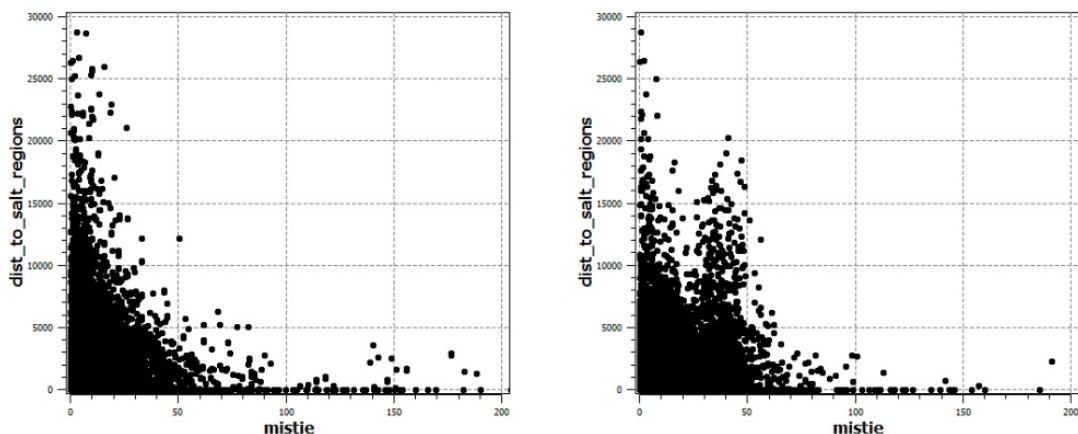


Figure 8: Cross plot of the map distance to the salt structures (vertical axis in meters) versus mistie for the Kr2 reflector (left) and the T1 reflector (right), given in milliseconds on the horizontal axis. Points falling onto a salt structure polygon have a distance of zero.



Further, as can be seen from Figure 9 the misties for the different reflectors are completely uncorrelated.

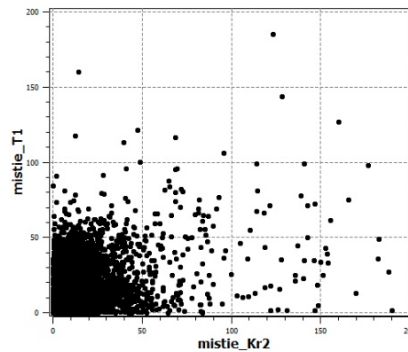


Figure 9: Crossplot for the misties of Kr2 against T1 for the points where both data are available (in milliseconds).

2.3.3 Uncertainty in seismic interpretation

One contribution to uncertainty from seismic imaging that is large but very hard to quantify is the uncertainty that is generated by the fact that the conceptual model, which should be applied by the seismic interpreter, is often not sufficiently known (see Figure 1, Step 2 in Chapter 1). For this reason, geoscientists use their training and experience (i.e., their prior knowledge) to apply a concept to the data in order to perform an interpretation (e.g. of seismic images) and, for example, to finally produce a geological or structural 2D or 3D framework model. However, this application of prior knowledge or assumption is often subject to uncertainty. This conceptual uncertainty e.g. comes into effect when a seismic image has to be interpreted but not many data such as sparsely distributed borehole data or other general geological constraints (e.g. tectonic setting, regional geodynamic history etc.), are available. Accordingly, conceptual uncertainty always includes methodologically based uncertainty due to data distribution, quality and quantity. This is especially important for the interpretation of 2D-seismic data. The first challenge is that the interpreters have to extrapolate their concept from one seismic line to the next. In addition, the lines often consist of different surveys, different ages and processing, and therefore also very different quality. This is especially important for the interpretation of salt structures, where an image of the salt structure flanks and top can change from line to line. Consequently, in such a multi-survey case the dependence of conceptual uncertainty is more obvious as in the case of uniform coverage by only one survey of same quality. One might think that the error caused by the application of wrong concepts is reduced by the acquisition of modern 3D seismic data. However, even the complete coverage with modern 3D seismic data does not guarantee the complete imaging of the subsurface in the same good quality and the avoidance of interpretation errors. With the increasing heterogeneity of the subsurface, only small impedance contrasts of the units under investigation and a complex sub-surface structure with diapirs and faults, a high degree of fuzziness in the data has often still to be accepted even with today's techniques. So, there are many different uncertainties that can build on each other.

Bond et al. (2015, 2008) have investigated this uncertainty coming from the ambiguity of seismic images and the influence that biases have on the results of the interpreters. They mainly differentiated following types of biases:



- Availability bias. The decision, model, or interpretation that is most readily brought to mind.
- Confirmation bias or/and hypothesis testing bias. To seek out opinions and facts that support one's own beliefs or hypotheses.
- Anchoring bias. Failure to move away from experts' initial beliefs, dominant approaches, or initial ideas.
- Optimistic bias or/and positive outcome bias. 'It won't happen to me' mentality or 'there is definitely oil in this prospect!'

Bond et al. (2007) suggest that an interpretation, and therefore the resulting initial geological framework model, is a fundamental source of uncertainty because it is dependent on the tectonic paradigm or concept used in its construction (i.e. the interpreters bias). As a consequence, Bond et al. (2007) also argue that conceptual uncertainty can be more important than the uncertainty inherent in the positioning of horizons or fault planes in a framework model or in the subsequent populating of these features with petrophysical properties. In order to illustrate consequences of conceptual uncertainty in seismic interpretation Bond et al. (2007) carried out an experiment with 412 subjects interpreting a seismic image that they generated artificially from a constructed and consistently restorable 2D geological section that has been generated using the software 2D Move (@Petroleum Experts, former Midland Valley).

The experiment showed that a large range of interpretations could result from a single data set. In this case, only 21 % interpreted the example in the right way and only 23 % found the given major faults strands in the image. In a later study, they further investigated the acquired data and showed that two main factors for finding the right interpretation are the breadth of tectonic education/knowledge (equivalent knowledge of different tectonic settings and how to interpret seismic data from this region) and the incorporation of evolutionary processes (e.g. kinematics) into the interpretation workflow. Bond et al. (2007) suggest that other factors, such as an individual's training and the techniques used to interpret the section, may have more influence on interpretational outcome than tectonic expertise.

In the experiments by Bond et al. (2007) users had no additional information, such as tectonic settings, geodynamic history or well information. Fortunately, in most of the cases such information is available.

The effect of the breadth of interpreters' education/knowledge on seismic interpretation was also investigated by Alcalde et al. (2017b). They used a classroom environment to investigate and show that the knowledge of a high variety of different structural fault models has an impact on the interpretation of a 2D seismic section, as the interpreters have more options to recognize or fit one of the different available models to the shown data, even to parts of the seismic section with lower image quality. Thus, one important factor seems to be to make the interpreter resilient to availability bias (for an overview of different biases in geosciences see e.g. Wilson et. al, 2019). This kind of uncertainty is hard to capture quantitatively. Possibly several interpretations which are each based on one of the different concepts could be made and then subsequently used in the 3D modelling phase in a Monte Carlo style process.

Another source of uncertainty in seismic interpretation is insufficient image quality, so that the seismic does not define geological features in a sufficiently unambiguous way in terms of course and extent. Schaaf & Bond (2019), for example, use a classroom environment in which 78

individuals interpreted the same region of a 3D seismic cube, in order to investigate the uncertainty in the interpretation of faults and horizons from 3D seismics. They show that the variability in the location of fault sticks can be correlated with the quality of the seismic image, which is assumed to be represented by the root mean squared amplitude (RMSA) of the image at the different locations. Alcalde et al. (2017a) describe a similar investigation for a 2D seismic section and show that the uncertainty in the interpretation increases when the contrast in the seismic image (here a grey-scale image) or the continuity of the reflectors decreases. Often uncertainty in seismic interpretation is a combination of the above-mentioned factors (limited information, image quality, structural complexity, interpreter's knowledge as well as other biases).

Several examples of the uncertainties that are inherent in seismic interpretations are given from data in the North Sea. In this area, salt structures are very common and many uncertainties in the interpretation are due to the limitations in the seismic imaging of these salt structures. Salt has a high seismic wave velocity (often more than twice that of surrounding sediments) which can result in strong refraction and reflection at the salt-sediment interface and energy loss of seismic waves. This in turn can result in an image with low quality of the immediate surrounding of the salt structures, especially below salt overhangs. A common consequence of this is that the ideal external form of the salt structure is not represented accurately in the seismic image, resulting in ambiguities in the interpretation of the external form of the salt structure. Although this also applies to faults and discontinuities especially in the basement of sedimentary basins, such effects are often less prominent in the seismic image for these linear structures than for salt structures.

Figure 10 shows a seismic section from the German North Sea Sector as an overview where different ambiguities may occur. The different examples that are visible in this section are now explained in more detail.

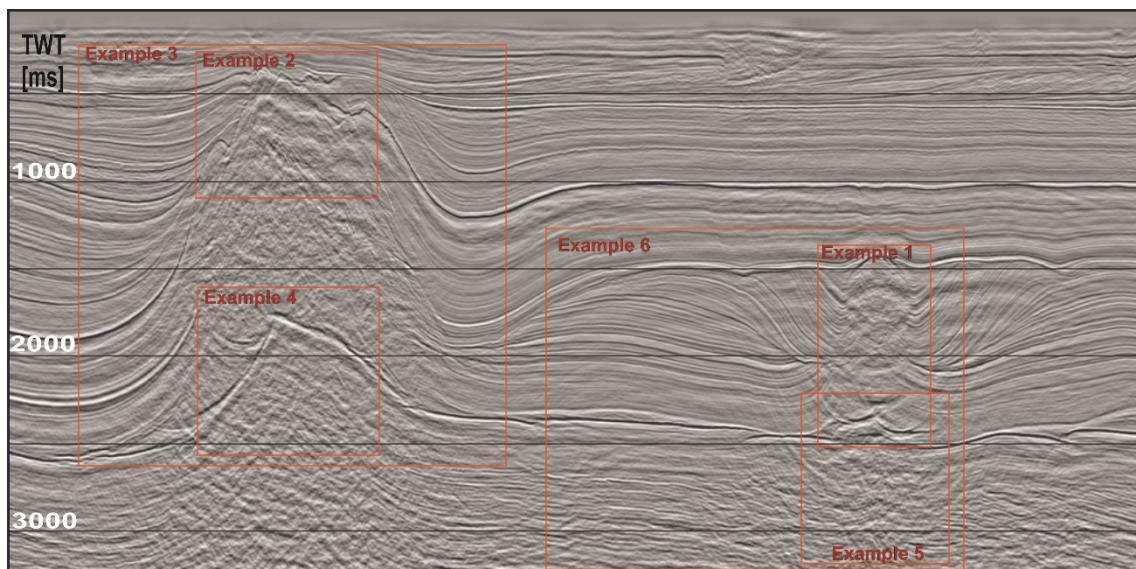


Figure 10: Exemplary (time-migrated) seismic section in the German North Sea (representative of many of the newer data sets in the German North Sea) that crosses salt structures and shows



different spots (red rectangles) where the interpretation is uncertain due to various reasons. The greatest interpretation uncertainties arise in the vicinity of salt structures and below them. However, sedimentary structures in the shallow overburden or steep faults in the basement, which are outside of the representation and processing focus of the seismic, are not sufficiently represented.

Example 1: Outer shape of salt structures

Figure 11 shows a subsection of Figure 10 along the smaller salt structure on the right side of the image. Besides the seismic image, no further information (e.g. well data) is available for the interpretation of the shape of the salt structure. For a clear interpretation of the outer shape of the salt structure and the bedding geometry along the salt-sediment-contact, the quality of the seismic image is not sufficient (Figure 11-a). Therefore, several interpretations of the salt structure shape are valid from given information. Figure 11-b and Figure 11-c show two conceptual end-members of salt-structure growth which have great impact on the resulting structural evolution of this salt structure. The two interpretations favour different modes of diapiric growth which implicate different rates of subsidence or salt movement and differences in the continuity of the processes. In both cases the diapir started as a reactive structure by extension of the sedimentary cover on top of the salt-layer, highlighted by the asymmetry in the pre-kinematic layers and the rollover below the „left“-rim-syncline. After that first reactive pulse, both interpretations differ in the details of rates of subsidence and salt-movement. In the case presented by Figure 11-b salt movement and the rates of filling the rim-synclines are partly out of balance. The following salt glaciers are formed or the diapir is covered by sediments of the expanding rim-synclines without stopping diapiric growth. The resulting growth pattern of the structure is also called Christmas-tree diapir. The example in Figure 11-c presents a more continuous growth history without periods breaking the overall long-lasting trend of diapiric growth. These examples both show two end-members of diapiric growth which are potentially imaginable in the structural setting of this region. However, comparison with similar structures in the region (important tool for proof of consistency) makes the interpretation in Figure 11-c more likely. Without additional information about the regional context, both interpretations represent "valid" solutions based on the given information. Thus, besides the interpretative uncertainty due to the insufficient resolution of the seismic, there is also a conceptual uncertainty. Nevertheless, if the geodynamic development history of the region is known, it can be used to further constrain the interpretation.

The low resolution of the seismic signal around salt structures is mainly due to problems and pitfalls associated with their imaging such as complex raypaths, seismic velocity anisotropy, P- and S-wave mode conversions, and reflected refractions. Jones & Davison (2014) give a comprehensive summary of numerous issues effecting the seismic imaging in and around salt bodies, and show different processing methods, such as Reverse Time Migration, which could improve the image quality. However, geological services often need to work with legacy data and so often do not have the option to use these techniques.

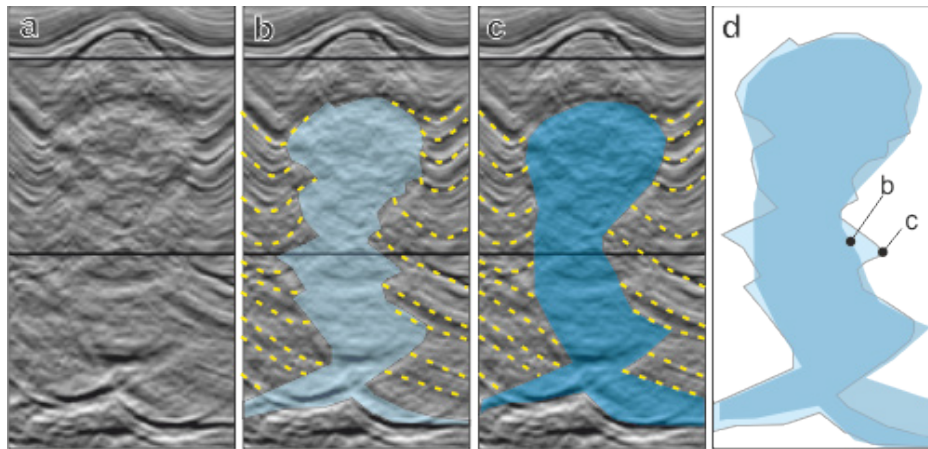


Figure 11: Seismic representation of a salt structure and possible interpretations of the salt structure (blue) and the surrounding sediments (yellow dashed lines) (b, c). d shows a comparison of the outer shapes of the structures in b and c. See Figure 10 for an overview of the seismic section.

Example 2: Crestal structures of diapirs

In Figure 12 the extract of the seismic section from Figure 10 shows the top part of a salt wall. In general, the crestal structure of a diapir is often very heavily deformed by forces accompanying the growth of the structure or act during salt withdrawal, as well as influenced by effects of subsrosion. The segmentation into several small and often deeply dipping faulted blocks (e.g. Yin et al., 2009) decreases seismic imaging and complicates the differentiation in main salt body, cap rock and adjacent sediments. Presumably, the interpreters oversimplify the salt cap structures, especially if the cap rock material is thin or shows similar seismic characteristics like sediments of the flank. Well explored structures onshore give an impression of the partly given complexity in the top of salt structures (e.g. Best & Zirngast, 2002). Figure 12-b and Figure 12-c show two possible interpretations of the salt structure example (in time domain). Due to the only moderate image quality of the 2D seismic line, some properties of the salt structure cannot be interpreted with sufficient certainty. Question marks about the interpretation persist with regard to

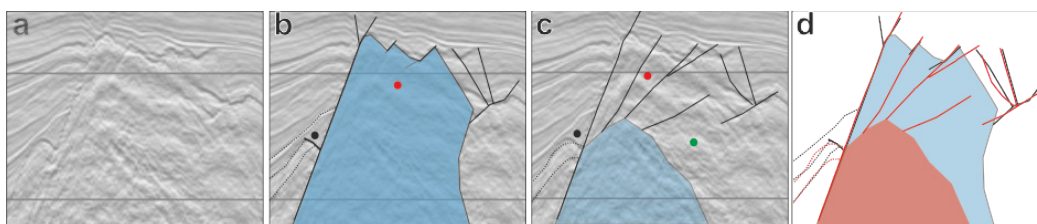


Figure 12: Seismic image of a salt wall top in the German North Sea, illustrating the difficulties in differentiating between salt body, cap rock and adjacent sediments. See Figure 10 for a full view of the seismic section.

- the structure of the sediment-salt contact (antithetic faults or rollover on the main fault; imaged in an overview scale in Figure 10) (black dot)
- the extent/thickness of the possible caprock (red dot)
- the age of the sediments covering the salt structure (green dot).



An incorrect interpretation of the top of the salt body leads to an incorrect representation of the geometry and thus of the geodynamic development history of the diapir. Due to former salt dissolution an anhydrite residue may have developed at the top/crest of a salt structure forming a thick anhydrite cap rock (up to several hundreds of meters). As a consequence, the “true” salt body geometry may be interpreted incorrectly (Figure 12). Additionally, the thickness of the cap rock has a significant influence on the depth representation of the salt body (or the change of shape/geometry of the salt body and underlying basement during the time-depth transformation) due to the physical properties of the evaporites and the resulting differences of the velocities between cap rock and the actual salt body (Table 1). The additional analysis of seismic velocities (if available in legacy datasets) could, however, provide the interpreter with valuable clues to limit its fuzziness in the interpretation (major differences in seismic velocities between rock salt, anhydrite and siliciclastics).

Example 3: Impact of a salt structure on the velocity field

Additionally, when a salt model is being built (e.g. for depth imaging), it is often assumed that the evaporite body is pure halite with a constant compressional wave speed of 4500 m s^{-1} . But almost all salt bodies contain additional evaporite minerals with significantly higher velocities than halite, such as gypsum or anhydrite and/or minerals with significantly lower seismic velocity, such as the K-Mg-rich mineral Carnallite, resulting in a distinct velocity anisotropy across the salt structure. As shown in Table 1, seismic velocities can vary significantly between typical evaporite minerals. However, larger deviations from the median of seismic velocities of 4500 m/s within the Zechstein salt bodies do not usually occur in the southern North Sea. This occurs only if instead of the thick main salt of the Staßfurt Formation younger Zechstein formations or even units of the salt-bearing Upper Rotliegend were included in the diapir formation or the rock salt from the Staßfurt formation were dissolved or eroded in earlier stages of salt structure evolution.

Table 1: Density and seismic velocity of typical evaporite minerals.

Mineral	Density (kg m^{-3})	seismic velocity (m s^{-1})
Halite	2200	4500
Gypsum	2300	5700
Anhydrite	2900	6500
Carnallite	1600	3900

Often seismic interpretation is performed in the time-domain, so the geometries of structures do not correspond to their real shape because of lateral distortions by lateral and vertical changes in seismic velocities. This can lead to significant differences in thickness of units with the depth or differences between real dip and apparent dip of structures in time domain (Figure 13). Experienced interpreters can handle such negative impacts on their interpretation but are not immune to misjudgement. A depth conversion without additional well control or additional velocity information could also ultimately lead to false assumptions. This issue is generally addressed during depth conversion of seismic data, where time units are converted to depth units. Another example of this salt body/cap rock/adjacent sediments differentiation problem for the Norwegian North Sea region is well illustrated in Jones and Davison (2014).

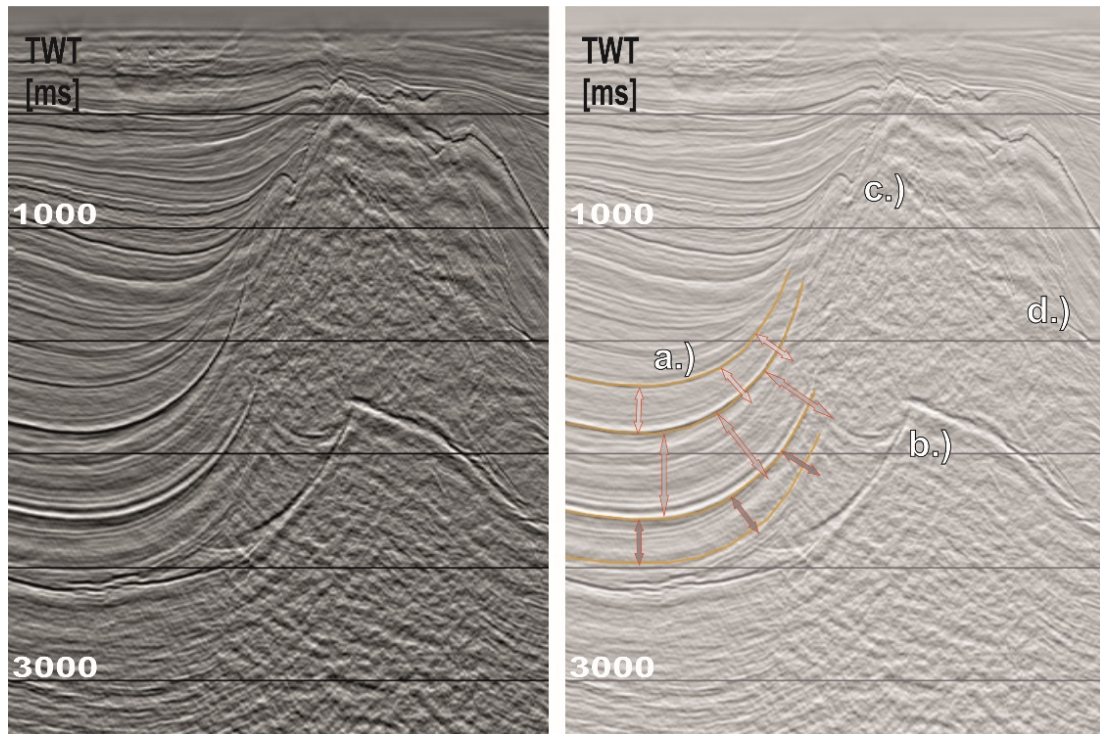


Figure 13: Seismic section across a salt wall and adjacent rim-synclines in the German North Sea, illustrating the difficulties in interpreting seismic sections in time and differentiating between (a) real thickness changes within an adjacent rim-syncline or the impact of increase of overall seismic velocities with depth; (b) a real horst structure limited by faults or a velocity pull-up structure beneath a salt structure; (c) real over-steepened structures or the influence of strong lateral changes in the velocity field; (d) effect of an unfavourable direction of the profile not being perpendicular to the strike of the salt flank or the real complexity of the flank. This can have a considerable effect on the quality of the seismic image. See Figure 10 for a full view of the seismic section.

Example 4: Effect of the velocity field on subsalt interpretation

Erroneous interpretations of a salt structure geometry and wrong assumptions for the lateral velocity changes above the basement may have considerable consequences for the interpretation of the sub-salt strata and structural elements. The influence/effect of the seismic velocity on the geometry of structures and strata is especially significant for structural interpretation below salt structures. Further, due to the strong reflections and refractions at the sediment-salt contacts, little seismic energy reaches the deep lying structures below the salt. This often leads to a generally lower resolution at greater depth (especially below salt structures). Thus, the geometry of sub-salt structures or basement faults is often not fully recognizable in seismic data and thus highly dependent on interpretation. Figure 14 illustrates this by showing three interpretations of the base salt. Independent of the different interpretations shown in Figure 14, the overview profile in Figure 10 shows a large offset in the depth trend of the base Zechstein in the area of the described salt structure. This is a strong indication of the presence of a large offset fault/fault-zone in the basement below the salt structure. This is also a good example of the fact that one should always create the structural

interpretation in the overall context of neighbouring structures in order to exclude wrong interpretations from the outset.

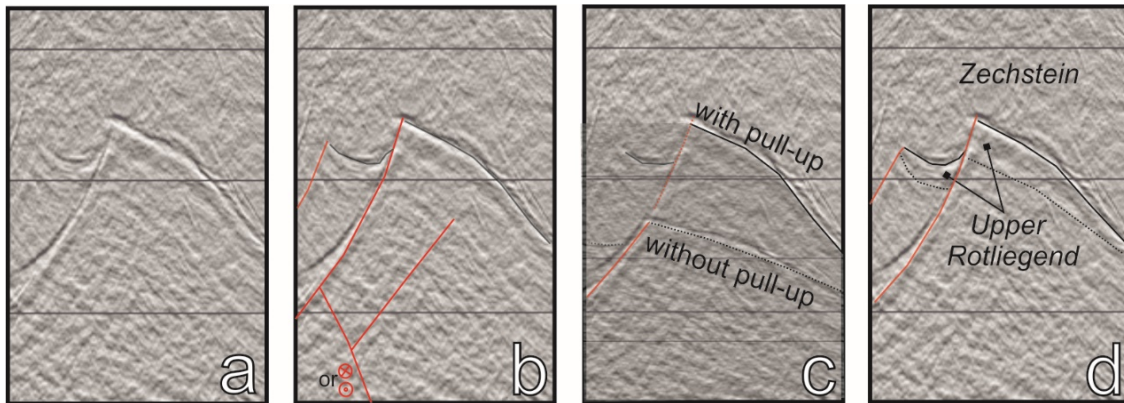


Figure 14: Example of different interpretations of the basement below a salt structure (see Figure 10 and Figure 13 for a full view of the entire structure). (a) seismic image; (b) the horst below the salt structure could be due to a complex wrench structure (transpressional/transensional) which was reactivated several times under different stress fields; (c) The basement bulge could have its origin in a velocity pull-up effect below the salt structure while only a minor offset fault structure exists below the diapir (the image in case c shows an overlay of two different stretches of the same image to outline the possible velocity pull-up effect); (d) the interpretation assumes additionally to major extensional faulting with only minor strike-slip component that salt from the Upper Rotliegend flows towards the highest point of the structure, increasing the differences in the structural gradients along the base Zechstein.

Example 5: Another example of interpretation of subsalt structures

As mentioned above, the seismic resolution is generally decreased at greater depth, especially below salt structures. As a consequence, interpretation of deep, sub-salt structures is therefore often subject to uncertainty. Figure 15 a-d shows four different interpretations of a basement fault below a minor salt structure (see Figure 10 for location). Each interpretation differs in fault geometry and/or fault kinematics and therefore the geodynamic history necessary for its development. Ideally, any interpretation should be in line with all available information regarding both the regional geodynamic development (i.e. fault kinematics) and resulting fault mechanical constraints, e.g. honour typical fault dip angles.

Example 6: Absence of additional information, e.g. wells

Uncertainty in seismic interpretation may not be due to decreased seismic resolution alone, but also to the absence of external stratigraphic constraints e.g. well constraints. Figure 16 shows an example where salt dynamic evolution and subsequent erosion resulted in isolated occurrences of sedimentary units again in the vicinity of salt structures. No well constraint exists and because seismic reflectors are restricted to those comparatively small areas, they cannot be correlated with surrounding reflectors / similar reflectors nearby. In this case the stratigraphic affiliation of the reflectors is uncertain. In the area of the southern German North Sea, this situation can be observed in several locations, especially affecting the interpretation of the Upper Middle Keuper and the transition of the Upper Keuper to the Lower Jurassic. Due to the

different, partly asymmetrical development of individual rim synclines and the resulting lack of connectivity, it is not possible to correlate the seismic reflectors from one area to another (or to areas which are constrained by wells). A stratigraphic interpretation and, in this case, the reliable identification of Jurassic sediments in these areas is not possible without major uncertainty.

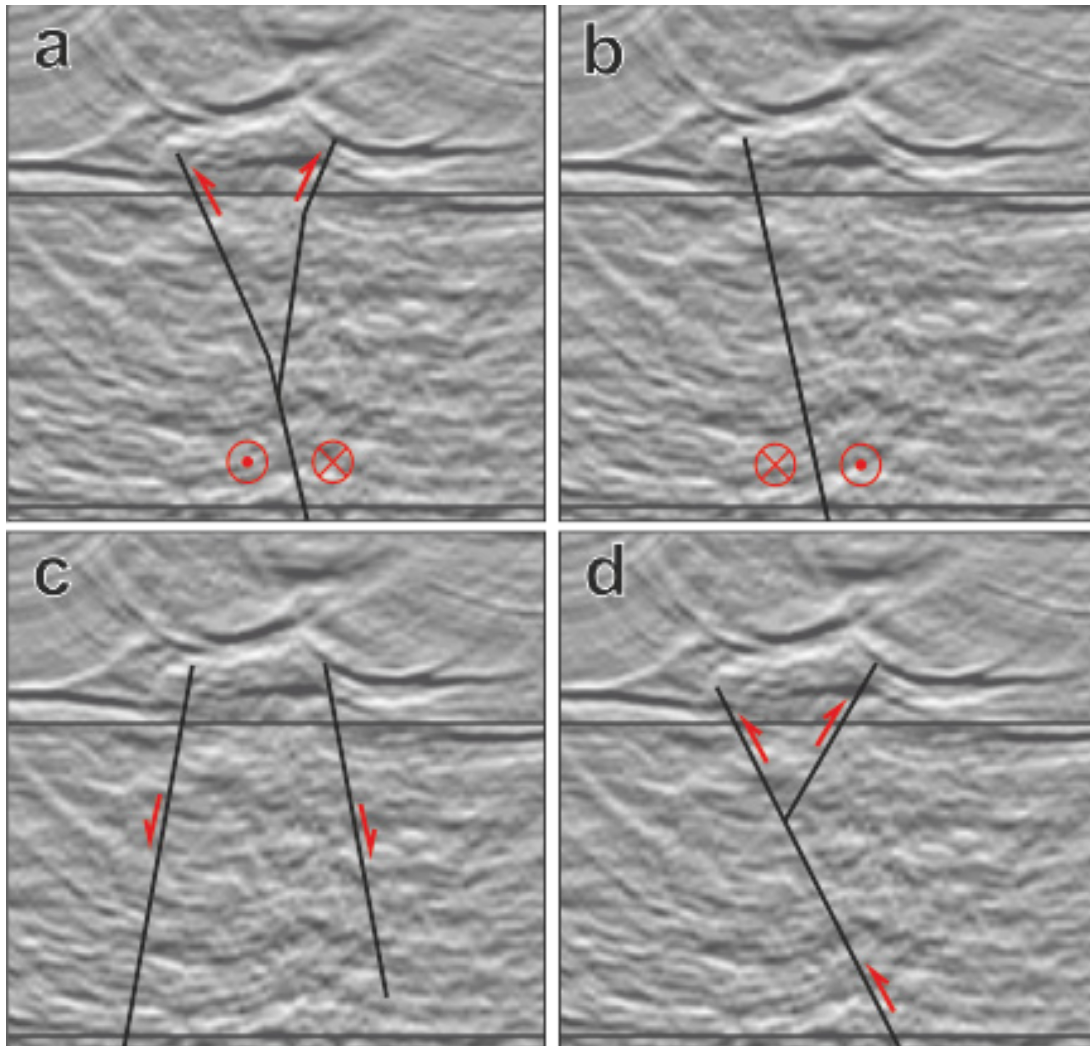


Figure 15: Due to generally lower resolution at greater depth, the geometry of sub-salt or basement faults is often not fully recognizable in seismic data. Without any further constraints (e.g. regional/sub-regional geodynamic and tectono-stratigraphic information/assumptions, comparison with neighbouring structures with a similar strike-direction), any of the four options of Figures a-d may be correct. In this specific case from the south eastern North Sea the (a) case of a transpressional fault zone and (d) a reverse fault are more unlikely.

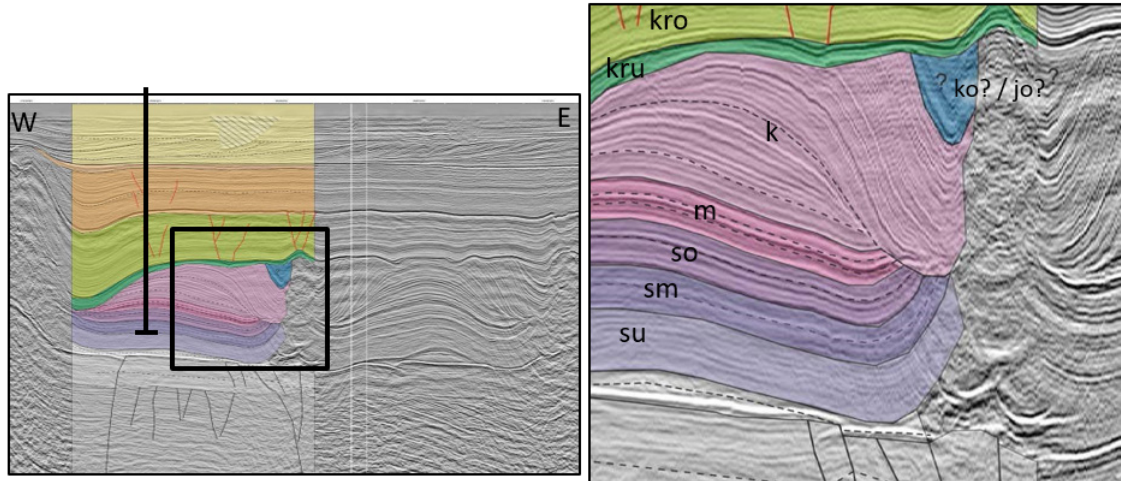


Figure 16: A rim syncline and adjacent turtle structure in the southern German North Sea. (left) overview view; (right) detail view of uncertain interpretation of sediments of the rim syncline. In the rim syncline and along the flanks of the turtle structure discontinued seismic reflectors can be observed, which are difficult to assign due to the lack of borehole constraints or ability to undertake a regional correlation with comparable reflectors.

2.3.4 Defining a velocity model with uncertainty, using check-shots at wells

The velocity model that is used for time to depth conversion of the structural model has a substantial impact on the depth of the horizons and structures in the final model and so it is important to find a way to assess the uncertainty in this model. One example of the generation of such a velocity model and assessment is the velocity model generated by TNO - Geological Survey of the Netherlands for depth conversion of deep subsurface models in the Netherlands. The layer cake velocity model was developed based on well velocity data (VELMOD-3). More material can be found at the corresponding Website: <https://www.nlog.nl/en/seismic-velocities>).

The used velocity dataset consists of sonic logs and checkshot data. Sonic data from different logging tools are available, often expressed in different formats like slowness, instantaneous sonic velocity and (calibrated) traveltime-depth (TZ) pairs. All raw velocity data were subject to quality control in terms of (velocity) data type and accompanying data unit. The dataset was checked per well for completeness. Wells without stratigraphic information were discarded. Wells without deviation data were considered to be vertical. The aggregated stratigraphic data have been quality checked on completeness and updated when necessary.

In VELMOD-3, an update of earlier versions, considerable effort was made to generate a (semi) automated workflow for processing the velocity, stratigraphic and directional well data. This made it possible to process the 3475 individual velocity data sources from a total of 1642 wells. Well plots of each data set allow the inspection of the data and detection of errors. The selection of a preferred dataset (if multiple datasets were available) per stratigraphic interval was based on a best statistical fit within the complete regional dataset.



The resulting preferred well data set is further used in model building of the layer cake velocity model. This velocity model assumes that the sedimentary layers, except for the Zechstein group, were subject to compaction due to sediment loading. Compaction results in an increase of compressional wave velocity and so the seismic velocity is assumed to increase linearly with depth:

$$V(x,y,z) = V_0(x,y) + K \cdot z$$

Where:

- $V(x,y,z)$ = velocity of the layer at depth z
- $V_0(x,y)$ = velocity at ordnance level
- K = factor determining the linear increase of velocity with depth

The Late Paleozoic Zechstein layer consists predominantly of high velocity carbonate and halite for which no clear relationship between seismic velocity and depth exists. The model parameter K is determined from the linear least squares relationship between the interval velocity (V_{int}) and mid-depth (Z_{mid}) of the layer. It is assumed that this parameter is independent of location.

CK Chalk Group

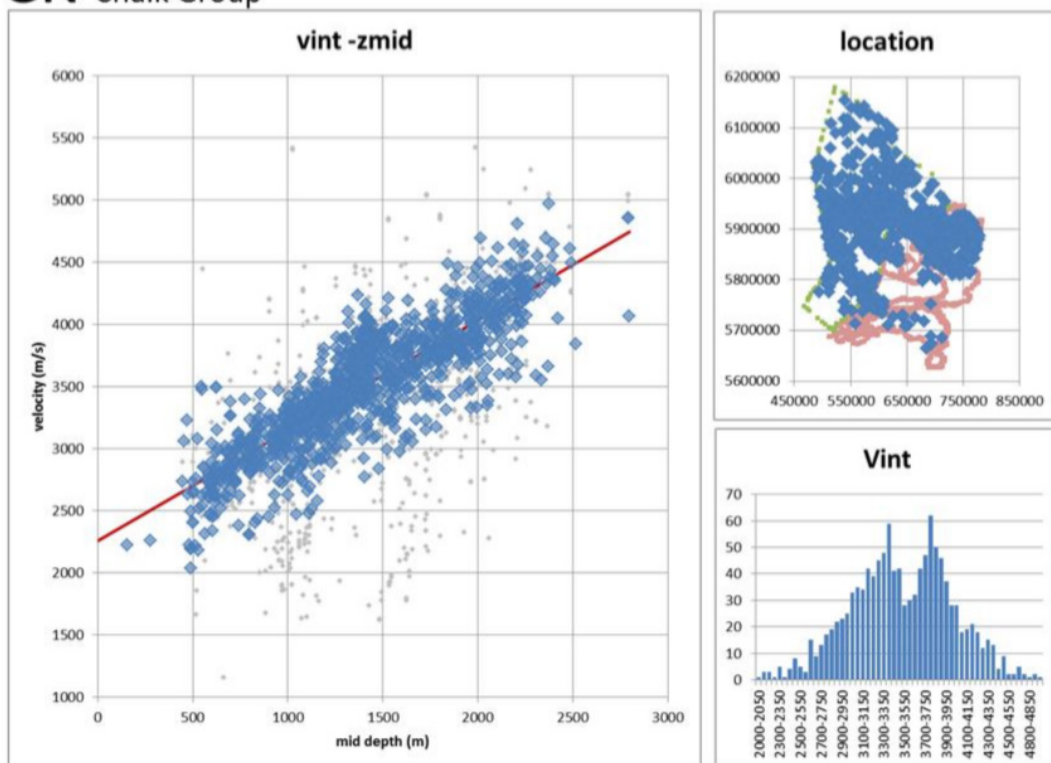


Figure 17: Example of a plot of interval velocity versus mid-depth to estimate k (from Pluymaekers et al., 2017).



The relationship between travel time in a layer and the thickness and depth of a layer for a linear increase of velocity is given by (compare with Japsen, 1993):

$$\Delta t = \int_{z_t}^{z_b} \frac{1}{V_0 + k * z} dz = \frac{1}{k} * \ln(V_0 + k * z_b) - \frac{1}{k} * \ln(V_0 + k * z_t)$$

This can be either rearranged to calculate the bottom depth of a unit (z_b) when the depth at the top (z_t), the travel time and k is known:

$$z_b = \frac{V_0}{k} * (e^{\Delta t * k} - 1) + z_t * e^{\Delta t * k}$$

Or it can be rearranged to determine the location dependent parameter $V_0(x,y)$ at borehole locations:

$$V_0 = \frac{k * (z_b - z_t * e^{\Delta t * k})}{e^{\Delta t * k} - 1}$$

This relationship implies that the model travel time between top (z_t) and base (z_b) of the layer equals the travel time Δt according to the sonic data.

The primary goal of VELMOD-3 is the construction of a regional velocity model for the use of time-depth conversion of regional seismic interpreted horizons. Consequently, interpolation of the well velocity data is needed to depth convert time grids. Simple kriging was applied in the gridding of the V_{int} and V_0 data points (Petrel Software). The grid cell size is 1000m x 1000m. A spherical variogram model was used with a relative nugget of 10% of the total variance. Variogram ranges were obtained through exploratory data analysis (Isatis statistic software).

Velocities for depth conversion of the Zechstein layer are based on interval velocities and a correlation between V_{int} and Δt -data in the wells. A provisional grid of interval velocities is built based on the travel times from seismic interpretation and the well- V_{int} Δt relation. Calculated differences between $V_{intprov}$ and $V_{intborehole}$ were kriged to obtain interpolated corrections of $\Delta V_{intprov}$. The final V_{int} -grid was obtained by subtracting the kriged differences from the $V_{intprov}$ -values.

When using Monte Carlo simulation to assess the uncertainty the velocity could be varied to generate the different realizations. Multiple V_0 maps can be generated by using Sequential Gaussian Simulation.

2.4 Uncertainty from acquisition to interpretation of the gravity data

In order to discuss the uncertainty that is involved in the use of gravimetric data and gravimetrical modelling in combination with petrophysical and geological data, and with the constraints of other geophysical information, it helps to look at a general workflow as shown in Figure 18, where the yellow boxes represent data (in the different levels of processing) and the blue ones the processes which are able to generate uncertainty. It is worth mentioning that this workflow is designed with a view to its application in areas where subsurface exploration data (e. g. seismic and wells) are scarce, but of course, when available, they would also be taken into account in the uncertainty analysis (see also deliverable 6.4 of the GeoERA project 3DGEO-EU, Pueyo et al, 2021). Therefore, three main pillars for the modelling of gravimetric data with their own sources of uncertainty are considered (level 1); gravimetric, geological and petrophysical



data that will propagate in further steps. Beyond that level, interactions (modelling) among all sources of information may happen in 2D and 2.5D (level 2) as well as in 3D (level 3) independently or in combination and thus, uncertainty of the structural models can be evaluated in 2D and 3D.

In level 1 (top of Figure 18), firstly the petrophysical properties of the different lithologies or geological units and their distribution are estimated from field (and laboratory) records, from well logs or harvested from databases. Secondly, structural, stratigraphic and cartographic features are acquired in the field and/or from data repositories. Thirdly and lastly in level 1, gravimetric data are measured in the field and processed and/or harvested from data bases. A first quality check and uncertainty assessment must be done already for this level, as the processing of the gravimetric data contains different types of uncertainties. Some of them are related to the acquisition of the data itself (imprecision in the measurement process, positioning of the stations), and others to the procedures for reducing the measured gravity data to obtain the observed gravity anomaly.

In level 2 the gravimetric data are processed to obtain the Bouguer anomaly that for upper crustal studies is separated in its regional and residual components. As an aid to interpretation, other techniques are used such as the Euler deconvolution, vertical and horizontal derivatives, etc. The usual way to interpret the data is obtaining a regular grid that is represented in a map. Further, cross sections are generated from the structural and stratigraphic information. Whenever possible, the cross sections are balanced, honouring basic geometric rules (see overviews by Groshong, 2006, Allmendinger, 2015 and López-Mir, 2019). Software packages allow density functions to be used that are deduced from petrophysical data, while other software packages only allow constant densities to be assigned. In any case, we always make sure that the cross sections for which the calculated gravity anomaly matches the observations, are consistent with each other. In this way, the seriated cross sections represent a plausible image of the subsurface.

Sequentially or alternatively (the 2D step may be skipped in areas with extensive or at least sufficient subsurface information), in level 3 an integrated 3D structural model is built merging all data together - the petrophysical and geological data (formation and structural trends, bed dips, stratigraphic thicknesses, etc.) together with the measured gravimetric field. The integration of the geological data to obtain the initial 3D geological model can be performed in several software platforms such as Skua-Gocad created by Emerson-Paradigm, Move by Petroleum Experts (former Midland Valley Ltd.) or Petrel by Schlumberger. The resulting 2D, 2.5D or 3D models will have geological (depth geometry, contacts, faults, etc.) and petrophysical attributes with their associated uncertainties derived from level 1.

Further processing during the generation of 3D models with attributes includes the explicit and implicit modelling and parametrization of the geometry (e.g. Skua-Gocad by Paradigm, Petrel by Schlumberger) and the forward modelling and inversion of potential field data; for example in GeoModeller (by Intrepid Geophysics), in IGMAS+ (by Schmidt et al., 2010) or in GM-SYS 3D (a module of Oasis Montaj from Seequent). Within the 3DGEO-EU project, 3D Geomodeller is mainly used by IGME (Instituto Geológico y Minero de España) to perform stochastic inversion and to allow for inverting the geometry, the density or both, and further GMSYS 3D is used



where the inversion is performed in the Fourier domain in order to invert the density or the geometry of a given layer.

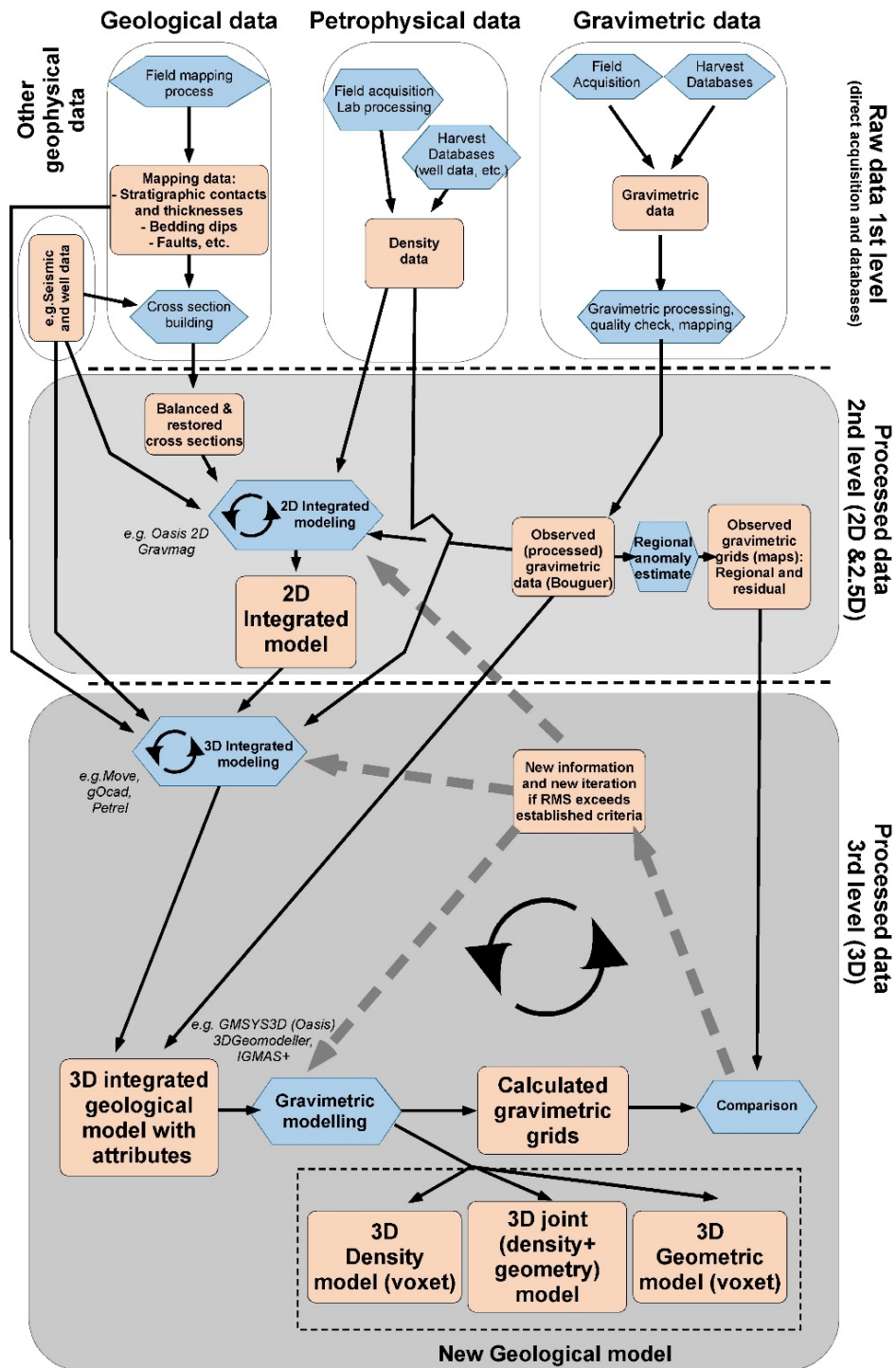


Figure 18: Generalized workflow for the use of gravimetric measurements and gravity modelling in order to improve the geological model.



The first step is to build up the geological model and add the physical properties, density in this case. Then we calculate its gravimetric response and compare it with the observed gravity anomaly. We modify the model, either “manually” (forward model) or “automatically” (inversion) until the pattern of the calculated anomaly fits the observed anomaly reasonably well. In order to analyze the uncertainty involved in the whole process, it is necessary to consider all three main sources of data and their related uncertainties: gravimetric, geological and petrophysical data as well as those sources which originated during the different levels of processing. Then, while integrating all together during the modelling process (2D, 2.5D and 3D, either forward or inversion), additional sources of uncertainty must be considered as well as the propagation of uncertainties derived from the lower levels to the final 3D geological model.

2.4.1 Uncertainty related to gravimetric data

The interpretation of gravimetric data itself contains uncertainties at different levels. Some of them are related to the acquisition of the data itself (imprecision in the measurement process, positioning of the stations), and others related to the procedures for processing the measured gravity data to obtain the observed gravity anomalies that are not always calculated using the same standard or take into account the same parameters (Seigel, 1995; Hinze et al., 2005). The semi-quantitative interpretation of the gravity data (Euler solutions, derivatives, etc.) and the gravity modelling (either forward or inversion) also contain uncertainties that are difficult to assess.

Besides, different levels of accuracy are required for surveys with different objectives (i.e. regional studies versus microgravimetric prospecting). The level of precision required will determine the field procedure and the level of accuracy of the corrections that are pertinent. Focusing on a given survey, instrumental errors and the data reduction procedures will require post-processing to estimate the associated uncertainties that propagate and accumulate into the final data. For example, Cattin et al. (2015) have developed a MATLAB software that allows the gravity data to be processed and the uncertainties to be obtained at the same time. At IGME, for example, the uncertainty is usually estimated by repeating a 10% of the survey and calculating the standard deviation of the differences between pairs of repeated measurements. However, before undertaking any joint interpretation, we have to bear in mind that the uncertainty level of the raw gravimetric data is significantly lower than other raw data sources (geological or petrophysical data).

2.4.2 Uncertainty related to geological data

Geological cross sections are keystones in 3D modelling, especially if they are balanced and restored. They represent the integration of several geological and geophysical data. With respect to geological data (see sections 2.1 and 2.2 for further details on borehole and seismic data and 2.4 for the uncertainty of field measurements), uncertainty mainly comes from the acquisition and analysis of the raw data needed for cross-section construction (implying natural, human, sampling quality and instrumental uncertainties; Bardossy and Fodor, 2011) and from the interpretation done when data are incomplete or scarce and are extrapolated at depth (implying conceptual uncertainties). The instrumental sensitivity conditions data accuracy of bedding attitudes, fault geometry and/or bed thicknesses. The choice of inappropriate outcrops and the natural variability of beds and faults due to, for example, thickness changes, stratigraphic tilted beds and geometrical variations of structures, constitute human and natural



uncertainties. To reduce them, a dense and representative sampling of structural data is fundamental to establish and individualize dip domains and properly apply existing fold and fault geometrical models (Groshong, 2006; Fernández et al., 2003). An uncertain structural model could be constructed that reflects these ambiguities (see Section 3 of this report).

Nevertheless, the exposure of geological elements is normally incomplete (Jones et al., 2004; Keffer, 2007; Lindsay et al., 2012) and a certain amount of interpretation is needed. For example, when dealing with shortening estimates from 2D sections, eroded or unknown subsurface cutoffs constitute a major source of uncertainty, as well as the occurrence of inherited extensional faults or salt structures later reactivated (Bulnes and McClay, 1999; Judge and Allmendinger 2011; Groshong et al., 2012). This likewise occurs when internal deformation (Mitra, 1994; Moretti and Callot, 2012; Sans et al., 2003) or when out-of-plane motions in the cross section are obviated (Pueyo et al., 2004; Sussman et al., 2012).

These sources of uncertainty have been partially studied but few of them quantified in previous work (see e.g. overviews by Judge and Allmendinger, 2011; Woodward, 2012; Lingrey and Vidal-Royo, 2015 and the previous section). Beyond these, a more severe source of uncertainty is related to the so-called “conceptual uncertainty” (Bond et al., 2007; Bond, 2015). The application of incorrect geological models when building cross sections (or 3D models) in areas with scarce and heterogeneous datasets can turn into totally erroneous interpretations. However, when these “wrong” models or sections are used to compute the potential field it is likely that the match to the measured potential field is worse than if the sections (or 3D model) are correct.

2.4.3 Uncertainty related to petrophysical data

Petrophysical data (in particular rock density, magnetic susceptibility and remanence), as one of the three keystones for the 3D modelling based on potential-field geophysical data, is a significant source of uncertainty due to the large natural variability of these properties in rock volumes (Henkel, 1994; Tenzer & Gladkikh, 2014; Schön, 2015; Enkin et al., 2020; among many others). Uncertainty analysis on density (and other petrophysical variables) from borehole logging data has been performed by the oil industry (Moore et al., 2011; Reichel et al., 2012); instrumental (measurements and calibration) and processing (correction and conversion processes) sources of error have been identified. However, much work still needs to be undertaken in relation to the estimation of accurate uncertainties derived from the natural variability, among other factors (Adams, 2005; Gaillot et al., 2019). Using outcrop samples, uncertainty related to the estimation method (usually the Archimedes principle) is usually small. Natural variability at outcrop and formation scales is very seldom determined, although both density and magnetic susceptibility and magnetic remanence vary very frequently in an order of magnitude of two or more on this scale. Uncertainty is estimated statistically using the standard deviation of the samples for each lithology. This variable has been used to narrow down the density assignation of density values during modelling (Köhler and Eichner, 1973).

In gravimetric modelling (from regional studies to micro-scales) petrophysical uncertainty is commonly obviated in many workflows, sometimes the raw data are poorly described in technical reports or scientific papers, and very often they are usually scattered, scarce and many times opaque. Sometimes, data from the literature (e.g. Schön, 2015) are assigned to rock



(lithological) formations for the 2D and 3D modelling of the observed gravimetric signal. When seismic velocities are available, densities may be obtained from them.

As adjusting the observed anomalies can be performed either by modifying the geometry, by modifying the petrophysical data for a given rock formation or by modifying both simultaneously, this ambiguity becomes an additional source of uncertainty. To reduce this ambiguity, the petrophysical information must be considered as primary and key data in 2D and 3D potential field modelling. Numerous samples for characterizing the natural density variability of the target formations have to be acquired directly from outcrops (and then processed in the laboratory) or harvested from databases (rock samples or well logging; e.g. Enkin, 2018; Pueyo et al., 2016). Further, density to depth relationships (from formation density logs) have to be considered during modelling. The final goal is to build robust histograms (i.e., characterizing the probability density function) for every modelled volume to constraint the mean density and its variability (both at surface and at depth) in order to be able to estimate a much more realistic uncertainty.

All in all, and to the best of our knowledge, the uncertainty related to the natural variability of petrophysical data (rock density, magnetic susceptibility and remanence) assigned to rock volumes has been very little evaluated. More has to be done concerning the quantification of the uncertainty derived from the petrophysical data. In our opinion, only the statistically robust characterization of the rock density of a target formation at the surface (and in addition at different depths if possible) is the only way to estimate the real impact of its natural variability on the derived uncertainty in the final 3D model.

2.4.4 Uncertainty related to gravity modelling (forward and inversion)

In addition to the inherent uncertainties that the three main sources of the input data add to the gravimetric modelling (observed gravity anomalies, geological and petrophysical data), other sources of uncertainty derived during the modelling process (2D, 2.5D and 3D) and for the interpretation of the final results have to be taken into account.

The method of construction of the initial geological model (2D, 2.5D or 3D) will generate its own uncertainty. This uncertainty will depend mainly on the scale of the study area, the size of the model, the accuracy of the geological input data and the algorithms used to build up the model. We have to bear in mind that the model represents a simplification of the actual geology to create a manageable model and this simplification is an important source of uncertainties.

Another source of uncertainties is due to the non-uniqueness of the gravimetric method (Skeels, 1947). The calculated anomaly from very different models can fit the same observed gravity anomaly, and therefore we have to find the model that is consistent with all the available geological and geophysical observations. Further, each software uses a different algorithm to calculate forward modelling and inversion (e.g. Parker, 1973, Tarantola, 1987a) which leads to different ways to assess uncertainties.

There are two main methods to estimate uncertainty in gravity modelling: through sensitivity tests (e. g. Ayala et al., 2003) or probabilistic approaches (e. g. Guillen et al., 2008). In the sensitivity tests, a parameter (geological boundary, density) is changed until the calculated anomaly does not fit the observations. In the probabilistic method, the parameters of the final model are given with a probability which can be regarded as the uncertainty of the parameter.



Some software packages allow using density functions that are deduced from the petrophysical data (e. g. GeoModeller or GM-SYS 3D), while other software only permits a constant density to be assigned to each lithology (e. g. GM-SYS or Gravmag). In that case we sometimes allow lateral variations of the density for the same lithology across parallel cross sections taking into account the standard deviation of the density assigned to that lithology. We always make sure that the cross sections whose calculated gravity anomaly match the observations are consistent with each other. In this way, serial (and balanced) cross sections represent a plausible image of the subsurface (e.g. Izquierdo-Llavall et al., 2019).

The forward modelling and inversion of the geometry and/or physical properties of the models is calculated using GeoModeller (from Intrepid Geosciences where the stochastic inversion can be estimated) or GMSYS 3D (from Seequent where inversion is carried out in the Fourier domain varying a lithological horizon or physical property one at a time). We consider that the calculated gravity anomaly matches the observed gravity anomaly and therefore the model is finished when the mean RMS of the difference between the observed and calculated values is small enough and the pattern of the calculated anomaly fits the observed anomaly reasonably well. There is not a “magic” RMS number: it varies depending upon the objectives, size of the study area and depth of investigation.

As has become fairly obvious from the previous subsections 2.3.1 to 2.3.4, a quantitative assessment of the uncertainty for the overall process is very complicated and there is no established general workflow for an assessment. An example of how an uncertainty assessment for the acquisition and interpretation of gravity data could be done practically within limits is given in Deliverable 6.4 on “Optimized reconstructions workflows and best practices in 3D modelling” of 3DGEO-EU’s work package 6.

2.5 Uncertainty of field measurements

Where outcrops are available, field measurements, such as the strike and dip of planes, play an important part and can be used by subsequent modelling workflows. Allmendinger et al. (2017) have done an assessment of the precision and accuracy of such measurements with a traditional compass (brunton compass) and Apple iPhones S6 and 7 running iOS 10.3 and two Apps, Stereonet Mobile, which they have developed themselves and FieldMove Clino from Midland valley. They show that the individual measurements have a limited precision and can easily scatter $\pm 2^\circ$ in strike and dip. Further the mean of a set of 40 measurements with each device on the same plane was different for the devices, showing that the accuracy is also between one and two degrees. In another experiment they measured planes in the limbs of a fold with the analogue compass and with their app. While the individual measurements were slightly different (the average mismatch was $3.2^\circ \pm 2.7^\circ$), the difference was not systematic and so the mismatches canceled out and the determined fold axis was nearly identical. Novakova & Pavlis (2017) assessed the precision of two Android devices, an Honor 3D smartphone and a Lenovo B8080-F tablet which use a different magnetic field sensor and accelerometer. For the B8080-F the sensor readings already turned out to be too unstable to give reliable results and so only the smartphone has been tested further. However, by subsequently comparing measurements of fractures taken with the FieldMove Clino app with analogue measurements with a Freiberg compass it is shown that the smartphone measurements exhibit a very wide scattering and systematic error. So, in conclusion it seems that the precision and accuracy depends very much



on the hardware and that it should be assessed before a new brand or type of smartphone with new types of sensors is used for field measurements. Midland valley itself recommends Apple devices for its FieldMove Cline app and states that it has observed that the variations in measurements on Android devices seem to be much larger, suggesting a lower quality of hardware in these devices.

Another way of determining structural data is the construction of a virtual outcrop and subsequent structural analysis of the generated model. Cawood et al. (2017) assess and compare the uncertainty by using three different techniques: Light Detection and Ranging (LiDAR) and the use of photogrammetric techniques on registered images (Structure from Motion, SfM) which have been acquired by an unmanned aerial vehicle (UAV, ASfM) and terrestrial with a handheld camera (TSfM). They undertook a structural analysis of the generated virtual outcrop and compared this to real data measured using an analogue compass-clinometer and a digital compass clinometer (FieldMove from Midland Valley on an iPad Air 3G). As the UAV could picture the structure from all sites and from top, the ASfM Method led to a reconstruction of 100% of the outcrop while the land bound systems, LiDAR and TSfM only achieved 69% and 78%. Comparing structural measurements on six control surfaces to the analogue compass measurements which were used as control data showed that the LiDAR-derived reconstruction best reflect the analogue measurements for the control surfaces with a maximum deviation of 5 degrees (between the poles). The TSfM method delivered the poorest results which was due to the fact that it could not reconstruct some of the control surfaces because of their hidden concave nature. The ASfM performed better but still did not achieve the quality of the LiDAR measurements. The digital compass clinometer showed dip deviations of 4° and azimuth deviations of up to 15°. The digital measurements also showed greater dispersion than the traditional measurements.



3 UNCERTAINTY AND 3D MODELLING

3.1 Overview

There are many textbooks on the computation of uncertain scalar data, such as facies or permeability, using geostatistical methods. See, for example, Isaaks & Srivastava (1989), Pyrcs & Deutsch (2014) or Remy et al. (2009). What is less commonly published are methods that deal with the estimation of the uncertainty of the geological structural model. One simple approach is to be aware that the uncertainty increases when moving away from the points where data are given. Siler et al. (2016), for example, compute a volume with the relative uncertainty for their structural model, ranging from 0 to 1, by first computing the distance to the data (seismic sections and boreholes) for each point and then fitting this distance to pre-defined logarithmic relative uncertainty curves. Further they assume that uncertainty increases with depth.

One of the most commonly used methods to estimate the uncertainty in geoscience 3D structural models is the use of Monte Carlo simulation which is sketched in Figure 19. For the input data, such as borehole markers for horizons or faults, their positional uncertainty is assessed, using a spatial probability distribution function. Using these distributions, a set of input data is generated using random sampling which is then used to generate a 3D model, using a 3D modelling software, such as Skua-Gocad or Petrel. This is done several times and so for each set of input data a corresponding geological 3D model, called a realization, is obtained which is slightly different to the other ones. Epistemic uncertainty, such as different possible interpretations of a seismic section, could be incorporated into the Monte Carlo approach by eliciting the probability of each different interpretation from experts, and generating a corresponding number of realizations for each interpretation. This would, for example lead to a higher uncertainty near faults for which the presence is uncertain, so that epistemic and aleatoric uncertainty add up. The different realizations must then be summarized in order to describe the geological subsurface as one model with uncertainty and different techniques are available by doing this e.g. visually or converting the surface based models to volume (voxel) models (see below). Pakyuz-Charrier et al. (2018) give a good overview of how this method could be applied to assess the uncertainty in structural models.

However, the use of this method requires that the necessary number of model realizations can be generated with an acceptable effort, ideally in some kind of (semi-) automatic way. One way to do this is the use of an implicit modelling approach as, for example, described in Lajaunie et al. (1997). Software that implements approaches like this is, for example, the Structure and Stratigraphy workflow in Paradigm's Skua-Gocad software, or the software GeoModeller (Calcagno et al., 2008). GeoModeller has, for instance, been used by Pakyuz-Charrier et al. (2018) to assess the influence that the uncertainty of the borehole path and the uncertainty of the location of stratigraphic interfaces within this borehole path has on the uncertainty of the course of stratigraphic interfaces and faults in a 3D Model. They further study the sensitivity of this uncertainty dependent on the dip of these interfaces.

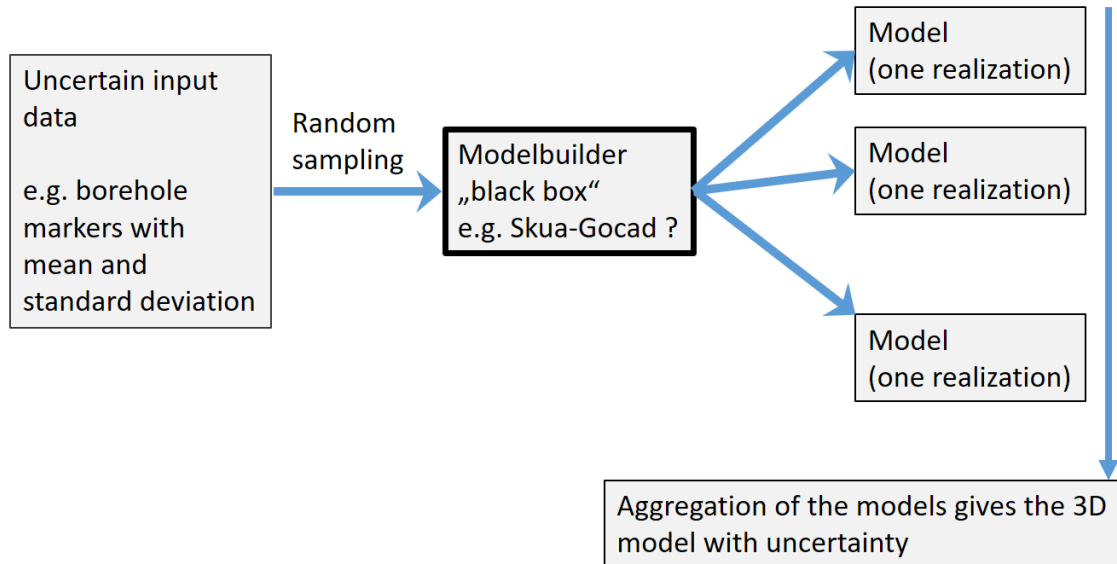


Figure 19: Sketch of the general idea behind an uncertainty estimation using the Monte Carlo technique.

SkuaGocad further provides a workflow, called structural uncertainty workflow, that creates multiple structural models based on the uncertainty provided for the input data. This workflow has been used by Schweizer et al (2017) in order to assess the structural uncertainty of a small 300x300x250 m large 3D model of a shallow geothermal reservoir in the city of Staufen, in the southwest of Germany, half way between Freiburg and Basel. They use this workflow for different models which are based on different amounts of input data. A basic model, a model that has been constructed using additional borehole information, a model that is built using additional information of 3D seismic and so on. They then investigate to what extent this additional information changes the overall structure of the model and improves the uncertainty within it. Wellmann & Regenauer-Lieb (2012) implemented an equivalent workflow in the context of GeoModeller to test their workflow using a simple test data set. Further, De la Varga et al. (2019) provide an open source Python based framework, called GemPy, which uses the technique described in Lajaunie et al. (1997) to generate the different models (realizations) of a geological model in an automatic fashion and allows the different models to be summarized into one model and thus provide an assessment of the uncertainty in the 3D model.

One example of a quantitative parameter that describes the uncertainty of a volumetric geological model is the information entropy (e.g. Wellmann & Regenauer-Lieb, 2012). Provided that different realizations of the structural model have been computed, it is possible to compute the geological unit to which each point or cell of a regular grid in each realization belongs. Subsequently the probability that a point belongs to a certain unit can be determined (for each unit). In order to express the uncertainty of a certain point or cell in a 3D geological model, the information entropy is then expressed as (e.g. Wellmann & Regenauer-Lieb, 2012):

$$H(x, t) = - \sum_i^N p_i(x, t) * \log(p_i(x, t))$$



Where x denotes the location, t could be time for a time dependent model and N is the number of different lithologies, or stratigraphic units that could occur at the given location. The information entropy will be between zero, when the point or cell with certainty belongs to a certain geological unit, and one, when it is very uncertain and it belongs to each unit with equal probability. The information entropy could then be visualized, together with the most probable unit in order to show where the model is highly certain and where not.

3.2 Estimating uncertainty for a regional 3D model in the Netherlands

One example of an uncertainty estimation using the Monte Carlo technique is the uncertainty assessment for the 3D model of the deep subsurface of the Netherlands, called DGM-deep (Kombrink et. al., 2012). The geological maps and more information can be found at <https://www.nlog.nl/en/geological-maps> and <https://www.dinoloket.nl/en/digital-geological-model-dgm-deep>. In order to assess the usability and reliability of this model a stochastic uncertainty workflow was developed as part of the modelling workflow.

DGM-deep is based on interpretations of publicly available 2D and 3D seismic survey data, combined with a variety of well data. The modelling workflow consists of building time maps for each horizon from the seismic interpretations, which are subsequently converted to the depth domain using an acoustic velocity model (VELMOD-3). After time-depth conversion a well-tie is applied such that the grid model in the depth domain acknowledges the well data. In a final step uncertainty of the model is addressed by calculating standard deviation grids resulting from stochastic simulations.

Stochastic modelling, in which multiple realizations for each horizon are generated, produces a Standard Deviation that gives information on the probability of the model (Figure 20). In the uncertainty workflow applied, accuracy and precision are combined. This is achieved by using the residual grids in the well-tie process, such that standard deviations between the well locations are centred around the well-tied depths surfaces (right part of Figure 20). This process does not, however, address the source of misties at the well location.

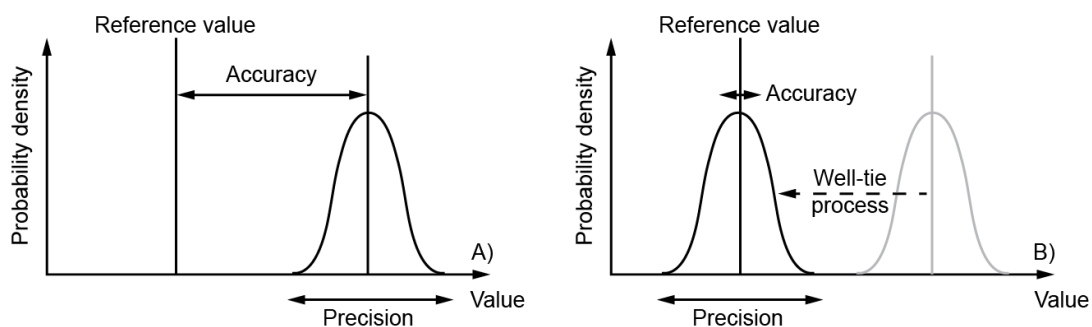


Figure 20: Left: Accuracy is the proximity of measurement results to the true value; precision, the repeatability, or reproducibility of the measurement. Right: Combined accuracy-precision workflow applied to DGM-deep (from https://www.dinoloket.nl/sites/default/files/file/dinoloket_toelichtingmodellen_dgm_deep_v4_notitie_uncertainty_20150327.pdf).



This stochastic uncertainty workflow follows the deterministic DGM-deep workflow in building time maps for each horizon from seismic interpretations that are subsequently converted to the depth domain, but also takes into account the potential error bandwidth for each data source. A stochastic simulation algorithm (Sequential Gaussian Simulation, SGS) is applied in order to generate multiple random realizations for each horizon, both in time and depth domain. Each horizon is then represented by its depth and the corresponding standard deviation (see Figure 21 for an example).

The workflow takes into account the following three error sources:

- **Data error:** This error takes into account any error related to the picking of a horizon within a seismic dataset and includes processing errors, vertical shifting errors and resolution errors. The data error increases with depth due to the decreasing quality of the seismic data. Also a larger error is assumed for picks traced from 2D seismic than those from 3D seismic. The data error is added as a noise factor to the original horizon picks using a short correlation distance (<1 km). Each realization is conditioned to the available data but varies within the error bandwidth away from the points.
- **Structural complexity:** This error is associated with the interpolation of the time maps. Areas characterized by low structural complexity and gentle features (e.g. platforms and highs) will produce small errors with interpolation, while in structurally complex areas (e.g. large fault offsets, salt doming) a significant error is introduced when large gaps exist between data points. The potential error that may be introduced with interpolation is determined by calculating moving standard deviation maps for the depth of each layer using a search window of 5x5 km. These maps represent the regional variation of potential interpolation error magnitude, which defines the bandwidth within which the SGS interpolation algorithm simulates the horizon depths. At the location of data points, the depth values will range within the data error bandwidth. Moving away from data points, the error gradually increases up to the maximum interpolation error set by the regionally varying structural error.
- **Velocity model error:** For each map of V_0 , a set of SGS realizations has been calculated using interpolation and variogram settings based on the VELMOD-3.1 model well-velocity data set.

Finally, the errors are combined to a joint depth error following these steps:

1. A random depth-dependent data error is added to all seismic horizon picks.
2. A random realization of a set of time domain maps for each horizon is obtained from the SGS interpolation of the seismic horizon picks (plus error) in combination with regional structural error maps.
3. A random realization of V_0 maps for each horizon is obtained from SGS interpolation of all available well velocity determinations.
4. A random realization of a set of depth domain maps is obtained from time-depth conversion of the realized time maps using the realized V_0 maps.

Kriging interpolation of residual well marker mismatches and the subsequent correction for these residuals ensures that the maps are conditioned to the wells used.

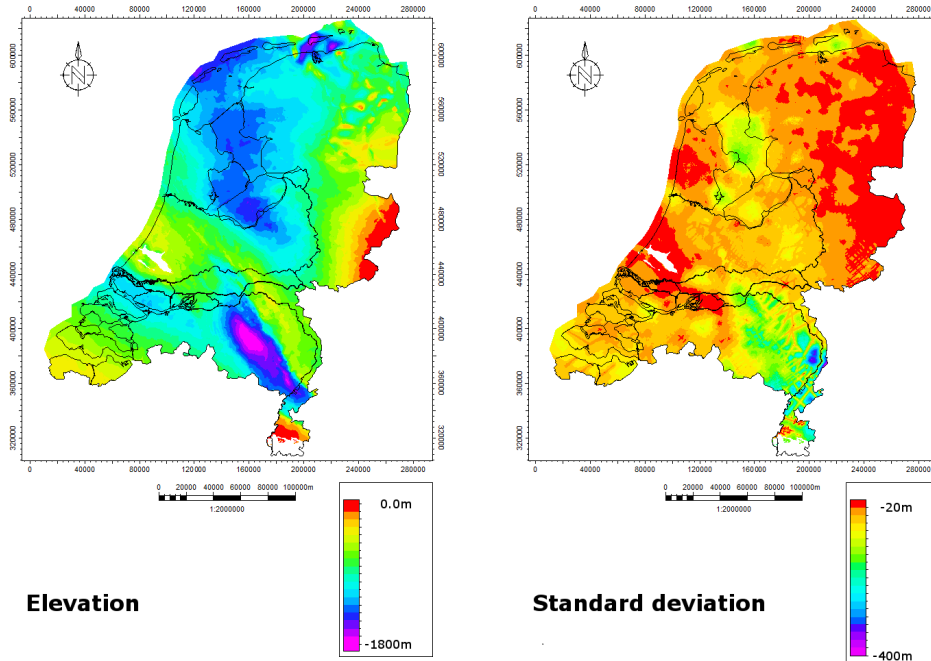


Figure 21: Exemplary side-by-side view for the elevation and its standard deviation (base of the North Sea Supergroup) within the Dutch DGMDeep model.

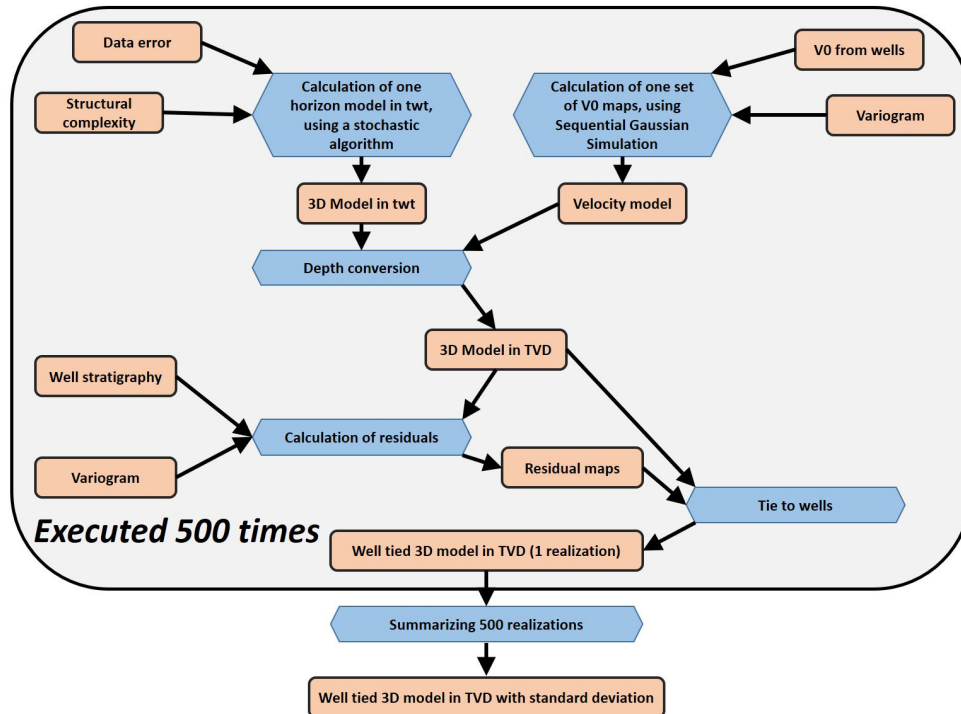


Figure 22: Overview of the workflow for uncertainty assessment of the regional geological model (DGMdeep) in the Netherlands, pictured as an event-driven process chain.



These steps are repeated until a set of 500 random realizations of time, velocity and well-tied depth maps are obtained. From this set of maps the final standard deviations are determined, representing the uncertainty of each mapping component (the likelihood that the real depth value lies between the estimated value plus or minus 1 times the standard deviation is approximately 64%, for a range of 2 times the standard deviation the likelihood is approximately 95%). Figure 22 shows the workflow as an event-driven process chain.

3.3 Uncertainty for a voxel based model with high data density

TNO - Geological Survey of the Netherlands builds and maintains several nation-wide geological models. While the deep model (see previous section) is represented by the geological interfaces (horizons), the shallow model, called GeoTOP, is represented as a voxel-based model, that schematizes the subsurface in 100 x 100 x 0.5 m voxels of up to a depth of 50 m below mean sea level. Each voxel is given an estimation of the stratigraphic unit as well as the lithological class. The current version of the GeoTOP model covers about 70% of the onshore part of the Netherlands, and is based on some 410,000 borehole descriptions that are available in this area. Below follows a concise overview of the GeoTOP modelling workflow, focusing on calculation of model uncertainty (see Figure 23). For more detailed information, please refer to Stafleu et al. (2010) and Stafleu & Dubelaar (2016).

2.5D Stratigraphic framework model

Constructing a model with lithological parameters requires more than blind interpolation of that parameter. GeoTOP is based on a stratigraphic framework model that is used to constrain interpolation of lithological information. GeoTOP uses automatic procedures to interpret the stratigraphy of borehole logs. Based on the depth of stratigraphic units in labelled boreholes, a stratigraphic framework model is calculated by an independent kriging interpolation of the depth of the base of each stratigraphic unit.

Uncertainty quantification of the depth of a stratigraphic unit is not an easy task, as quite a number of sources can be identified that may influence the uncertainty. First there is the stratigraphic labelling of borehole information, which is based on geological expertise. The construction of a geologically plausible stratigraphic 3D model then requires additional information based on expert geological knowledge such as the location of paleo-valleys, general geological trends in data-sparse areas, and depositional extent of sediments. With all this information imposed on the kriging interpolation, the kriging variance will not be able to provide a very useful estimation of the overall uncertainty. Gunnink et al. (2010) suggest a cross-validation-based approach to assess the uncertainty. The general idea of this approach was to leave out each data point – one at a time – and to estimate the variable at that location with the remaining data points. The difference between the true and the estimated variable at each location is used to quantify a so-called ‘regional’ standard deviation (the uncertainty outside of the variogram range of data locations). This regional standard deviation is lowered near data locations, by a factor determined by the normalized kriging variance. This method, used in a modified form (Dabekaussen & Hummelmann, 2021), benefits from quantifying the overall magnitude of uncertainty by cross-validation, while retaining the influence of the variogram to determine fine scaled variation in uncertainty at locations in proximity to data points.



3D voxel model

With the boundaries of the 2.5D framework model used to constrain interpolation, the 3D voxel model is now populated with estimates of lithological class. These estimates are calculated using the stochastic simulation technique Sequential Indicator Simulation (SIS; Goovaerts, 1997), that allows the construction of multiple, equally probable, 3D realisations of the model. The probability of occurrence of each lithological class within a voxel is then calculated from the stochastic model realisations by simply dividing the number of times a particular lithological class is assigned to a voxel by the total number of realisations. Note that this procedure produces a partial uncertainty of the lithological class, as SIS is performed without taking into account the uncertainty of the underlying stratigraphic framework model.

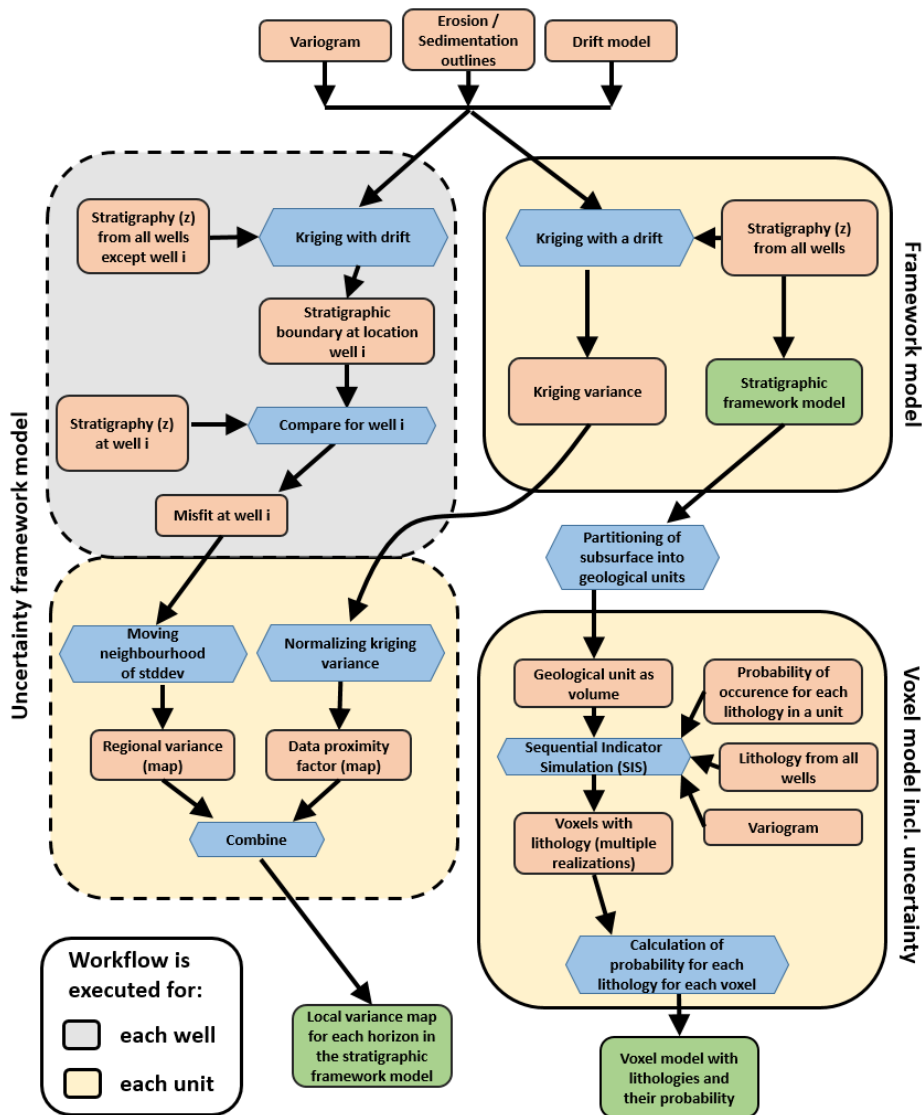


Figure 23: Workflow for the uncertainty estimation of GeoTOP, the shallow geological model of the Netherlands.



Visualisation of uncertainty

For a 1D vertical voxel stack, probabilities of lithological class can be displayed in a single bar graph, thus showing a probability distribution and hence model uncertainty (see Figure 24). Similar displays are possible in visualisations of virtual boreholes (i.e. vertical stacks of voxels). However in 2D visualisations, for instance a vertical cross-section through the voxel model, it is no longer possible to show all probabilities in a single view: the user will always be presented with one of the probabilities at a time.

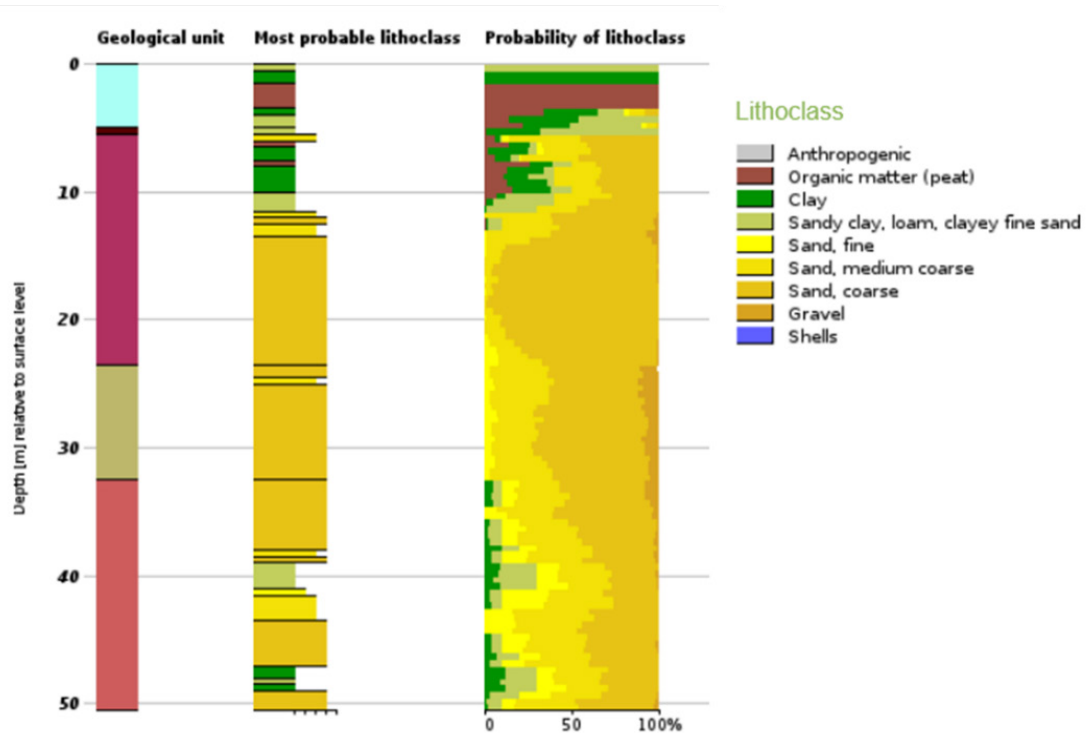


Figure 24: Visualisation of the geological unit, most probable lithoclass and model uncertainty of the lithoclass prediction, shown for a vertical voxel stack. The most probable lithoclass indicated in the middle column has been determined by using an averaging method which finds the optimum threshold where the ratio between lithoclasses is equal to the ratio in boreholes (see Soares, 1992).

To solve this problem, the concept of information entropy (Wellmann & Regenauer-Lieb, 2012) is used as a measure of uncertainty in 3D models (Stafleu et al., 2021). The information entropy of a voxel is a single value ranging from 0 to 1 that can easily be calculated from each of the probabilities of the lithological classes:

$$H(x, t) = - \sum_{m=1}^M p_m(x, t) * \log p_m(x, t)$$

where x denotes the location, t the time, and M the number of lithologies. An entropy value of 0 means that there is no model uncertainty (all model runs result in the same lithological class),

whereas a value of 1 occurs when all lithological classes have the same probability. Values in between 0 and 1 account for both the number of lithological classes with a probability higher than 0 (the more classes, the higher the entropy) and the differences amongst the probabilities (the greater the differences, the lower the entropy).

Figure 25 shows the information entropy of the lithological classes in a fence diagram cut through the GeoTOP voxel model. The diagram shows areas that are strongly influenced by single boreholes as vertical zones of low entropy. In addition, we can distinguish homogeneous stratigraphic units dominated by a single lithological class. In general, entropy increases with depth as data density decreases. Similar 3D displays can be made for the information entropy or model uncertainty of stratigraphic units.

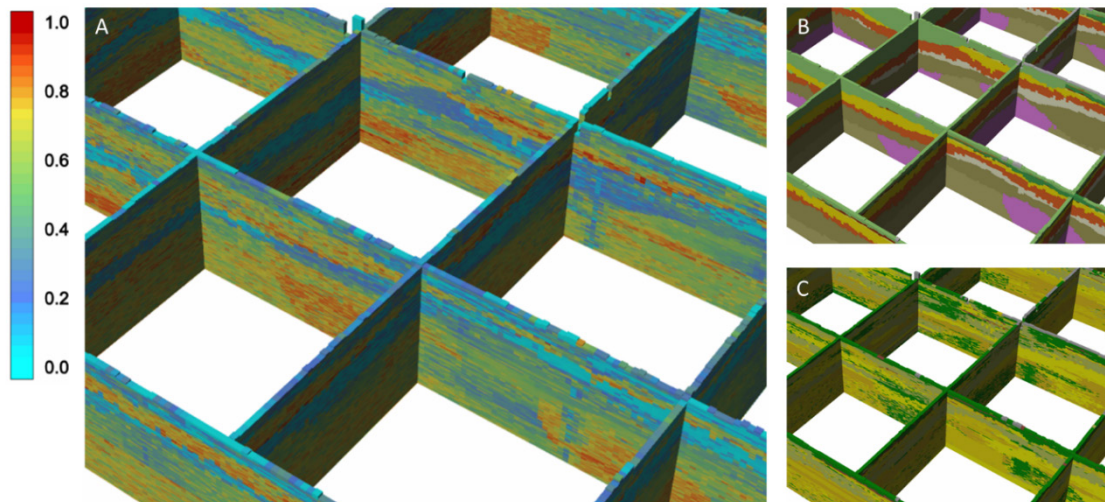


Figure 25 (A): Model uncertainty (information entropy) of lithological classes in a fence diagram through the GeoTOP voxel model, with entropy values ranging from 0 (blue) to 1 (red); (B): stratigraphic units of the model; (C) lithological class.

3.4 Estimating uncertainty for a model with low data density in geologically complex regions

In contrast to the previous example from the Netherlands, geological models in the Czech Republic are mainly based on scarce and heterogeneous data, as there are often only a few deep boreholes available and few geophysical data, such as reflection seismics in particular modelled regions. Further the geology in the Czech Republic is mainly built by crystalline units exhibiting several ductile deformation phases and magmatic intrusions, which involves a high degree of complexity and is less continuous and so mathematically less predictable than sedimentary environments. For this reason it would be very hard and unreliable to use automated methods of model building based on Geostatistics or to use Monte Carlo techniques. Instead the 3D geological models of regions of interest are generated manually, based not only on input data, but also on the field experience and relying on a particular model-based interpretation,



assuming e.g. a certain tectonic regime or deformation style. The uncertainty within such models is, apart from small-scale mineral deposits or reservoir models generated by mining companies, neither evaluated nor shown to the users and stakeholders. In order to change this, the Czech Geological Survey (CGS) is developing a workflow to assess and visualize the uncertainty in these models (Staněk et al, 2019). This method assesses 3 sources of uncertainty (local lithological complexity, distance to faults and so-called general uncertainty - a coefficient that increases with depth) while the resulting uncertainty decreases in the vicinity of available data (boreholes, geophysical profiles and possible other data sources).

As a first step in the uncertainty estimation, the original 3D geological model that is represented by mesh surfaces (horizons and faults) is rasterized and represented as a voxel-based volumetric model. This voxelized (and thus slightly simplified) model is then used for the subsequent computations and for the uncertainty visualization. Subsequently the three different sources of uncertainty are evaluated for each voxel:

1. Uncertainty due to local lithological complexity

In order to find a quantitative measure for uncertainty that is due to the structural complexity we use a principle published in several studies, e.g. by Brus (2014) for the 2D case or by Wellmann & Regenauer-Lieb (2012). As an indicator of the uncertainty of the boundaries of rock bodies and the lithological complexity, we chose spatial entropy $H(S)$. Brus (2014) states that the founder of the concept of entropy, C. E. Shannon (Shannon and Weaver, 1949), defined entropy as follows: for a system with a finite number of possible states $S \in \{s_1, s_2, \dots, s_n\}$ and the probability of their occurrence $P(s_i)$, the information entropy is defined as:

$$H(S) = - \sum_{i=1}^n P(s_i) * \ln(P(s_i))$$

This formula looks quite similar to the one given by Wellmann & Regenauer-Lieb (2012). They state that the minimum value is 0, because $\log 1 = 0$ and $\lim_{x \rightarrow 0} (x \log x) = 0$ which is possible to prove with L'Hopital's theorem (see Ben-Naim, 2008) and that the logarithm can be generally taken with any base, depending on the applied unit of information (in our case number of rock types). In contrast to them, we always use a natural logarithm in our calculation and then normalize results by dividing by $\ln(n)$, instead of changing the logarithm base.

Therefore, the information entropy is minimal if all probabilities $P(s_i)$ are equal to zero, except for one, which takes the value 1. It must therefore hold: $H(S_{\min})=0$ just when $\exists P(s_k)=1$ and $P(s_i)=0$ for $\forall i \neq k$. It can also be shown that the entropy is maximal, when the probabilities of occurrence of exclusive states are the same (the distribution is uniform): $H(S)_{\max} = \ln(n)$, that is exactly the case when: $P(s_i) = 1/n$ for all s_i . When the entropy decreases from $\ln(n)$ towards 0, the overall information grows, and vice versa. Entropy is the mean value of the information content to eliminate uncertainty, which is given by the finite number of mutually exclusive phenomena (here the individual rock types).

The calculated information entropy according to the above equation is a modified so-called Shannon index (Jenness et al., 2011 in Brus, 2014), which takes values ranging from 0 to \ln



(n) where n is the number of unique categories (rock types). The degree of uncertainty in the range from 0 to 1 is then obtained by dividing the calculated entropy by $\ln(n)$. The degree of the so-defined uncertainty then ranges from 0 (a very credible part of the model) to 1 (a very vague part of the model).

The calculation of entropy is executed for each cell in the 3D grid of a geological voxel model, using a given point neighbourhood, based on the equation above. The neighbourhood is defined as the set of size N , containing all N voxels with their centre in the sphere of given radius that has its centre in the middle of the voxel for which the entropy is evaluated. The probability $p_i = n_i/N$ is the ratio of the number of voxels with the rock-type i (n_i) to the total number (N) of voxels in the evaluated neighbourhood. This algorithm could be modified - for example, to increase uncertainty with depth by increasing the radius of the evaluated spherical neighbourhood with depth.

2. Uncertainty due to the presence of faults

The uncertainty that is due to the presence of faults is assigned based on the distance from a voxel to fault planes. In the geological model we differentiate 3 categories of brittle tectonic structures based on their size and importance - local minor faults, local major faults and regional faults. The fault uncertainty algorithm differs from the rock uncertainty calculation. It introduces a manually defined distance (radius of influence) of each category of faults and, because of the unknown or uncertain dip the uncertainty of the fault location at the highest level (just below the Earth surface) and at the lowest level (bottom of the fault or of the model). These values are manually set by the geologist in charge and/or the modeller. If more faults occur in the evaluated voxel neighbourhood, the highest value of fault-related uncertainty for the voxel is taken.

3. Adding of so-called general uncertainty

Subsequently, the so-called "general uncertainty" (a value of a minimum uncertainty, increasing with depth) and the local reduction of uncertainty (increased credibility) in the vicinity of documented boreholes and available other data (geological, geophysical sections etc.) are calculated, according to the input parameters specified by a geologist in charge. The so-called "general uncertainty" expresses the fact numerically that without extensive exploration works even the surface geology is often uncertain (inaccurate location of lithological boundaries, interpretative location of faults, omission of smaller rock bodies or rock bodies with little contrast for classical geological mapping techniques, ambiguous interpretation of shallow geophysics, etc.). General uncertainty can be input as polygons that allow an expert estimate to be applied in order to differentiate areas with generally better and worse data coverage (mainly extent of geological maps of a different quality and with a varying degree of detail) in relation to the geological complexity of the area.

Finally, the three different sources of uncertainty are combined. In order to merge the values of the different types of uncertainties in each voxel of the 3D grid, the conjunction of the particular uncertainties in the voxel is calculated as the maximum of the individual uncertainties (e.g. Vondrák, 2009). Figure 26 shows a diagram of the workflow.



Pilot area for testing the methodology

As a pilot area for testing the methodology to determine and visualize the data uncertainty, we chose a 3D geological model from the western part of the Bohemian Massif, with dimensions of about 20x15x1.5 km. This model was selected due to its high variability in geological structure and its good coverage by available archived data. The 3D geological model is composed of meshes that represent fault planes and boundaries of rock bodies (see Figure 27). The model has been first cut into 14 horizontal sections at 100 m vertical intervals using the software MOVE. The 2D horizontal sections contain polygons of rock types and fault lines that are topologically corrected in ArcMap and subsequently rasterized into 2D grids with a cell size of 50x50 m. So that except a variably thick surface layer, each voxel had size of 50x50x100m.

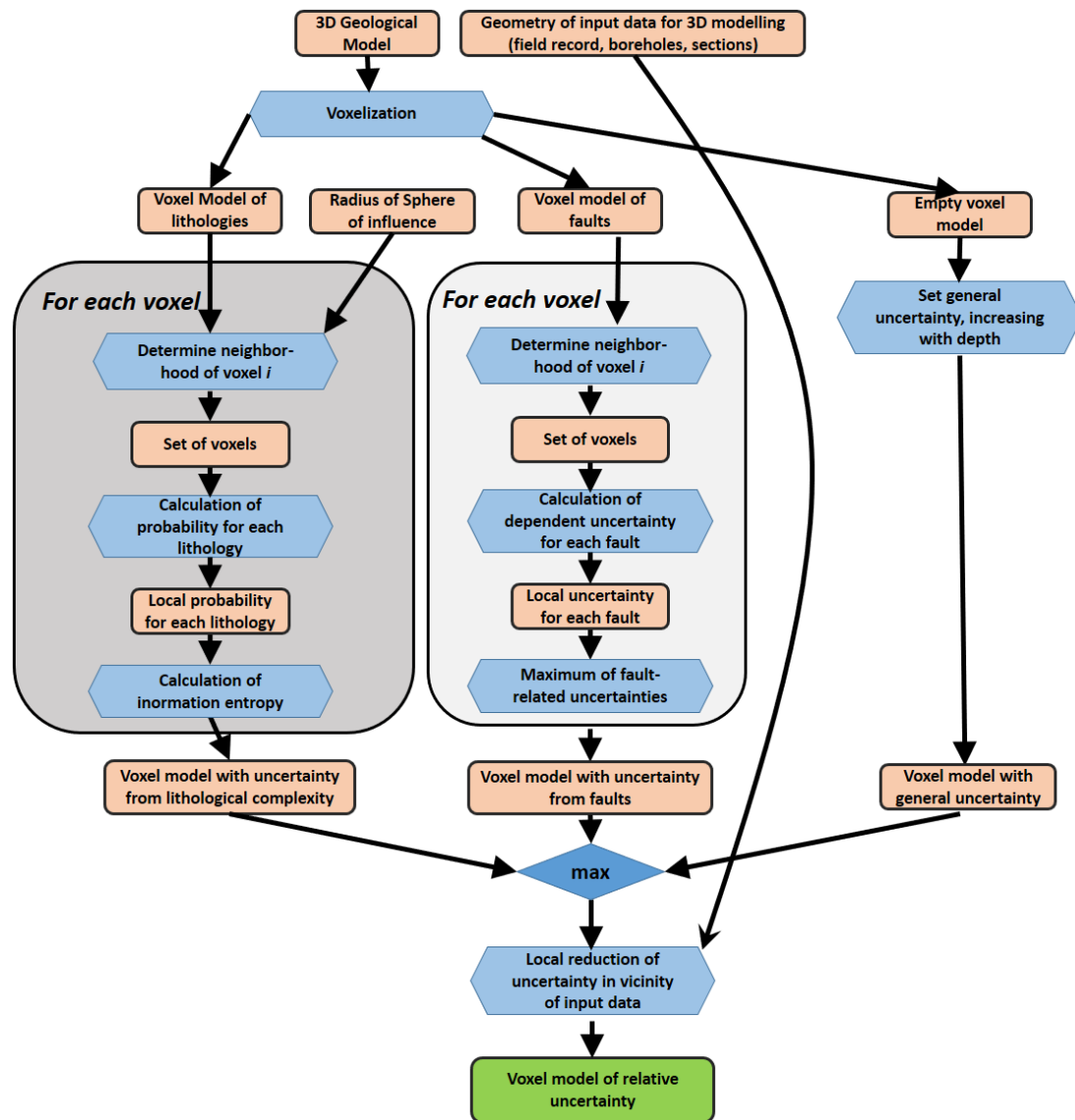


Figure 26: Workflow for uncertainty estimation of geological voxel models as applied by the Czech Geological Survey.

Subsequent to this rasterization process the different steps to assess the uncertainty are executed as described above. As a radius for defining the neighbourhood of each voxel 150 m have been chosen, eventually with depth-related increase up to 350m radius at model base. Further the influence of the faults has been defined by the geologists to lie in a range of 250 m to 550 m. The algorithm can further be modified for example to increase depth uncertainty by increasing the radius of the spherical neighbourhood. In the test example, the 3D grid of rock types is created from 14 horizontal sections ranging from -900 to +300 m a.s.l. For higher levels up to the surface (roughly between 400 and 600 m a.s.l.) the 15th layer is introduced which contains the rock bodies and faults from the surface geological map.

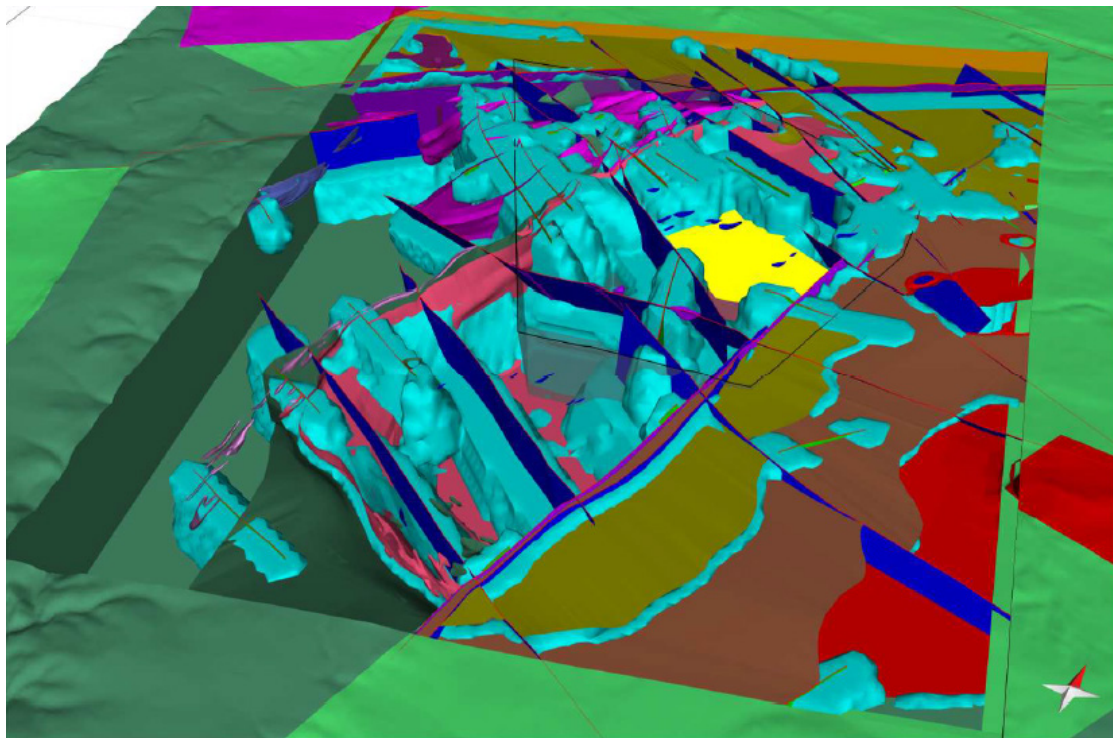


Figure 27: Surface-based representation of the geological model for which the uncertainty is to be assessed. The resulting relative uncertainty of 0.35 is visualized as a light blue isosurface, encapsulating regions of uncertainty higher than 0.35.

The resulting voxel model with uncertainty has been visualized using the software Voxler (see Figure 28). It should be noted that the calculated uncertainty values do not have an exact quantitative meaning. Due to the heterogeneity of the input data and many necessary expert estimates of the input parameters of the calculation, we do not expect to find a universal calculation for absolute values of uncertainty regarding 3D models of geologically complex terrains in the future. However, the resulting values can be used to compare the relative uncertainty in the individual parts of a single model / across a single generation of methodically uniform models, and are primarily aimed for users who do not have the necessary deep general and regional geological knowledge to be aware of these uncertainties on their own – e.g. for

engineers and designers of underground constructions to stress out domains where more exploration should be realized before starting the construction works.

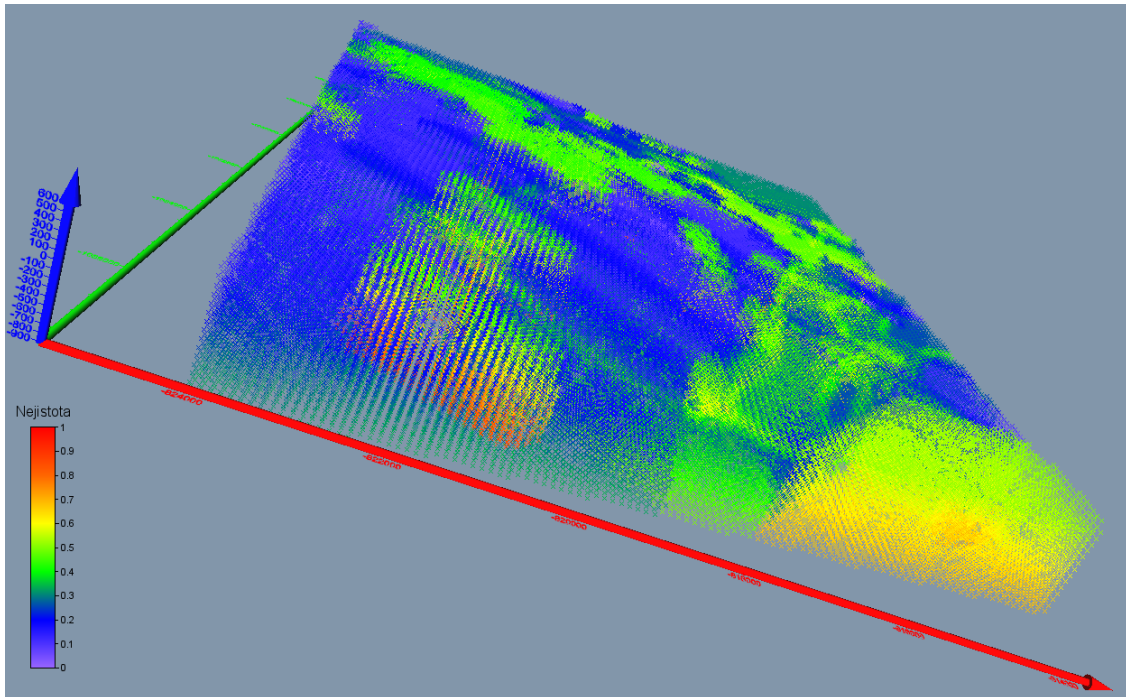


Figure 28: Visualization of bulk uncertainty in Voxler using the ScatterPlot rendering. The values represent the maximum of the uncertainties based on rock types, fault categories and general uncertainty that has been locally reduced by certainty imposed by presence of input data - exploration boreholes and geological/geophysical sections.

4 USE OF UNCERTAIN STRUCTURAL MODELS

The 3D structural models that are generated, e.g. by the geological survey organizations, are not only used for communication purposes but also to subsequently execute process simulations, to estimate reserves or to estimate environmental risks. Bárbara et al (2019) for example investigate the impact of the structural uncertainty on the gross rock volume in two oil reservoirs. Witter et al (2019) give an overview of how the uncertainty can be evaluated and used during geothermal planning and development.

When 3D geological models have been generated for further analysis, such as the simulation of fluid flow, not only the position and course of the different structures (e.g. faults and horizons) are important, but also how the different geological bodies are connected. The relationships among the geological bodies, seen as discrete elements of the model, are known as the topology of the model. Thiele et al. (2016a) give an overview of the description of topology in geological models and discuss how this topology could be determined for voxel models and for maps, how it can be visualized, and give some examples of how it could be used. Further they show how



the influence of the uncertainty in the geological structure can be analyzed by quantifying the topological uncertainty (Thiele et al, 2016b).



5 REFERENCES

- ADAMS, S. J. (2005, January). Quantifying petrophysical uncertainties. In: *SPE Asia Pacific Oil and Gas Conference and Exhibition*. Society of Petroleum Engineers
- ALCALDE, J., BOND, C. E., JOHNSON, G., ELLIS, J. F., BUTLER, R. W. H. (2017a): Impact of seismic image quality on fault interpretation uncertainty? *GSA Today*, 27 (2), pp. 4-10, <https://doi.org/10.1130/GSATG282A.1>
- ALCALDE, J., BOND, C. E., JOHNSON, G., BUTLER, R. W. H., COOPER, M. A., ELLIS, J. F. (2017b): The importance of structural model availability on seismic interpretation, *Journal of Structural Geology* 97, pp. 161-171, <https://doi.org/10.1016/j.jsg.2017.03.003>
- ALLMENDINGER, R.W. (2015). Modern Structural Practice. A structural geology laboratory manual for the 21st century. <http://www.geo.cornell.edu/geology/faculty/RWA/structure-lab-manual/>
- ALLMENDINGER, R. W., SIRON, C. R., SCOTT, C. P. (2017): Structural data collection with mobile devices: Accuracy, redundancy, and best practices, *Journal of Structural Geology* 102, pp. 98-112, <https://doi.org/10.1016/j.jsg.2017.07.011>
- AYALA, C., TORNÉ, M. AND POUS, J. (2003): The lithosphere-asthenosphere boundary in the western Mediterranean from 3D joint gravity and geoid modelling: tectonic implications. *Earth and Planetary Science Letters*, 209, 3-4, pp 275-290
- BADDELEY, M. C., CURTIS, A., WOOD, R. (2004): An introduction to prior information derived from probabilistic judgments: elicitation of knowledge, cognitive bias and herding. In: Curtis, A. & WOOD, R. (eds): *Geological Prior Information: Informing Science and Engineering*. Geological Society London, Special Publications, 239, pp. 15-27.
- BÁRBARA, C. P., CABELLO, P., BOUCHE, A., AARNES, I., GORDILLO, C., FERRER, O., ROMA, M., ARBUÉS, P. (2019): Quantifying the impact of the structural uncertainty on the gross rock volume in the Lubina and Montanazo oil fields (Western Mediterranean), *Solid Earth* 10, pp. 1597-1619, <https://doi.org/10.5194/se-10-1597-2019>
- BÁRDOSSY, G., & FODOR, J. (2001): Traditional and new ways to handle uncertainty in geology. *Natural Resources Research*, 10 (3), 179-187.
- BEN-NAIM, A., (2008): *A Farewell to Entropy*. World Scientific, Singapore. 384 pp.
- BEST, G., ZIRNGAST, M., (2002): Die strukturelle Entwicklung der exhumierten Salzstruktur „Oberes Allertal“. Bericht der Bundesanstalt für Geowissenschaften und Rohstoffe (BGR), Hannover, Germany, 110p.
- BOND, C. E., SHIPTON, Z., JONES, R., BUTLER, R., GIBBS, A. (2007): What do you think this is? “Conceptual Uncertainty” in geoscience interpretation, *GSA Today* 17 (11), pp. 4-10. DOI: 10.1130/GSAT01711A.1
- BOND, C., SHIPTON, Z., GIBBS, A.D. & JONES, S. (2008): Structural models: Optimizing risk analysis by understanding conceptual uncertainty, *First Break*, Vol. 26 (6). DOI: 10.3997/1365-2397.2008006



- BOND, C. E., LUNN, R. J., SHIPTON, Z. K., LUNN, A. D. (2012): What makes an expert effective at interpreting seismic images? *Geology* 40, pp. 75-78.
- BOND, C.E. (2015): Uncertainty in structural interpretation: Lessons to be learnt. *Journal of Structural Geology* 74, pp. 185-200. DOI: 10.1016/j.jsg.2015.03.003
- BRUS, J. (2014) Visualization of uncertainty in environmental studies. PhD Thesis, Palacky University in Olomouc (in Czech), 175 pp.
- BULNES, M. & McCLAY, K.R. (1999): Benefits and limitations of different 2D algorithms used in cross-section restoration of inverted extensional faults: application to physical experiments. *Tectonophysics* 312, p. 175-189.
- CALCAGNO, P., CHILES, J. P., COURRIOUX, G., GUILLEN, A. (2008): Geological modelling from field data and geological knowledge Part I. Modelling method coupling 3D potential-field interpolation and geological rules, *Physics of the Earth and Planetary Interiors* 171, Elsevier, pp. 147-157.
- CATTIN, R., MAZZOTTI, S., & BARATIN, L. M. (2015). GravProcess: An easy-to-use MATLAB software to process campaign gravity data and evaluate the associated uncertainties. *Computers & geosciences* 81, 20-27
- CAWOOD, A. J., BOND, C. E., HOWELL, J. A., BUTLER, R. W. H., TOTAGKE, Y. (2017): LiDAR, UAV or compass-clinometer? Accuracy, coverage and the effects on structural models, *Journal of Structural Geology* 98, pp. 67-82, <https://doi.org/10.1016/j.jsg.2017.04.004>
- COHEN, K.M., FINNEY, S.C., GIBBARD, P.L. & FAN, J.-X. (2013; updated): The ICS International Chronostratigraphic Chart. *Episodes* 36, pp. 199-204.
- CURTIS, A., WOOD, R. (2004): Optimal elicitation of probabilistic information from experts. In: Curtis, A. & Wood, R. (eds) *Geological Prior Information: Informing Science and Engineering*. Geological Society London, Special Publications, 239, pp. 127-145.
- DABEKAUSSEN, W., HUMMELMAN, H.J. (2021): Uncertainty of the geological framework model of the Netherlands. 82nd EAGE Conference & Exhibition, Amsterdam, Netherlands, Extended Abstracts.
- DE LA VARGA, M., SCHAAF, A., WELLMANN, F. (2019): GemPY 1.0: open source stochastic geological modelling and inversion, *Geoscientific Model Development* 12, Copernicus Publications / European Geosciences Union, pp. 1-32. DOI: 10.5194/gmd-12-1-2019
- ENKIN, R. J. (2018). The Canadian Rock Physical Property Database: first public release. GSC Open File 8460, 60p. <https://doi.org/10.4095/313389>
- ENKIN, R. J., HAMILTON, T. S., & MORRIS, W. A. (2020): The Henkel Petrophysical Plot: Mineralogy and Lithology from Physical Properties. *Geochemistry, Geophysics, Geosystems* 21(1), American Geophysical Union (AGU). <https://doi.org/10.1029/2019GC008818>
- FERNÁNDEZ, O., MUÑOZ, J. A., & ARBUÉS, P. (2003). Quantifying and correcting errors derived from apparent dip in the construction of dip-domain cross-sections. *Journal of Structural Geology* 25(1), p. 35-42.



FRANZ, M., BACHMANN, G.H., BARNASCH, J., HEUNISCH, C. & RÖHLING, H.-G. (2018): Der Keuper in der Stratigraphischen Tabelle von Deutschland 2016 - kontinuierliche Sedimentation in der norddeutschen Beckenfazies (Variante B). *Z. Dtsch. Ges. Geowiss.* 169, pp. 203-224.

FRICKE, S., SCHÖN, J. (1999): *Praktische Bohrlochgeophysik*, Enke Verlag, 254p.

FRODEMAN, R., (1995): Geological reasoning: Geology as an interpretive and historical science. *GSA Bulletin* 107 (8), pp. 960-968.

GAILLOT, P., LEWANDOWSKI, J., & NURSAIDOVA, R. (2019): Uncertainty Analysis in Formation Evaluation: Rationale, Methods and Examples. In: SPWLA 60th Annual Logging Symposium. Society of Petrophysicists and Well-Log Analysts. 24 pp.

German Stratigraphic Commission (ed.; editing, coordination and layout: Menning, M. & Hendrich, A.) (2016): *Stratigraphic Table of Germany 2016*, Potsdam (German Research Centre for Geosciences).

GeoMol (2021): www.geomol.eu. For 3D visualization of the Swiss part see e.g. <https://viewer.geomol.ch> [last accessed June 2021].

GOOVAERTS, P. (1997): *Geostatistics for Natural Resources Evaluation*. Oxford University Press, New York, 483 pp.

GROSHONG JR, R. H., WITHJACK, M. O., SCHLISCHE, R. W., & HIDAYAH, T. N. (2012): Bed length does not remain constant during deformation: Recognition and why it matters. *Journal of Structural Geology* 41, p. 86-97.

GROSHONG, R.H. (2006). *3-D Structural Geology - A Practical Guide to Quantitative Surface and Subsurface Map Interpretation*, second ed., Springer-Verlag, 400 pp.

GUILLEN, A., CALCAGNO, P., COURRIOUX, G., JOLY, A., LEDRU, P. (2008): Geological modelling from field data and geological knowledge: Part II. Modelling validation using gravity and magnetic data inversion. *Physics of the Earth and Planetary Interiors* 171, 1-4, pp. 158-169. <https://dx.doi.org/10.1016/j.pepi.2008.06.014>

GUNNINK, J., MALJERS, D., HUMMELMAN, J. (2010): Quantifying uncertainty of geological 3D layer models, constructed with a-priori geological expertise. 14th Annual Conference of the International Association for Mathematical Geosciences, Budapest.

HENKEL, H. (1994): Standard diagrams of magnetic properties and density — a tool for understanding magnetic petrology. *Journal of Applied Geophysics* 32(1), pp. 43-53.

HINZE, W.J., AIKEN, C., BROZENA, J., COAKLEY, B., DATER, D., FLANAGAN, G., FORSBERG, R., HILDENBRAND, T., RANDY-KELLER, G., KELLOGG, J., KUCKS, R., LI, X., MAINVILLE, A., MORIN, R., PILKINGTON, M., PLOUFF, D., RAVAT, D., ROMAN, D., URRUTIA-FUCUGAUCHI, J., VÉRONNEAU, M., WEBRING, M. AND WINESTER, D. (2005): New standards for reducing gravity data: The North American gravity database. *Geophysics*, 70, pp. 125-132.

HISS, M., NIEBUHR, B. & TEIPEL, U. (2018): Die Kreide in der Stratigraphischen Tabelle von Deutschland 2016 (STD 2016). *Z. Dtsch. Ges. Geowiss.* 169, 225-246.

INGLIS, T. (1987): *Directional Drilling*, Graham & Trotman, London, 260pp.



- ISAAKS, E. H., SRIVASTAVA, R. M. (1989): An Introduction to Applied Geostatistics, Oxford University Press, 561pp.
- IZQUIERDO-LLAVALL, E., AYALA, C., PUEYO, E. L., CASAS-SAINZ, A. M., OLIVA-URCIA, B., RUBIO, F., ... & GARCÍA-CRESPO, J. (2019). Basement-Cover Relationships and Their Along-Strike Changes in the Linking Zone (Iberian Range, Spain): A Combined Structural and Gravimetric Study. *Tectonics* 38(8), pp. 2934-2960.
- JAPSEN, P. (1996): Influence of Lithology and Neogene Uplift on Seismic Velocities in Denmark: Implications for Depth Conversion of Maps, *AAPG Bulletin* 77 (2), AAPG, pp. 194-211.
- JONES, I. F., DAVISON, I. (2014): Seismic imaging in and around salt bodies, *Interpretation*, Vol. 2, No. 4, Society of Exploration Geophysicists (SEG), <http://dx.doi.org/10.1190/INT-2014-0033.1>
- JONES, R. R., MCCAFFREY, K.J.W., WILSON, R.W., HOLDSWORTH, R.E. (2004) Digital field data acquisition: towards increased quantification of uncertainty during geological mapping. Geological Society of London, Special Publications 239, pp. 43-56.
- JUDGE, P. A., & ALLMENDINGER, R. W. (2011): Assessing uncertainties in balanced cross sections, *Journal of Structural Geology* 33(4), pp. 458-467.
- KAHNEMAN, D. (2011): Thinking, Fast And Slow, Penguin Books, 2012, 499pp.
- KAHNEMAN, D., SIBONY, O., SUNSTEIN, C. R. (2021): Noise – A Flaw in Human Judgement, Little, Brown Spark – Hachette Book Group Inc., New York, 454pp.
- KEEFER, D.A. (2007): A Framework and methods for characterizing uncertainty in geological maps. In: Thorleifson, L. H., Berg, R. C., Russel, H. (Convenors), Three-Dimensional Geologic Mapping for Groundwater Applications Workshop Extended Abstracts, Denver, Colorado. <https://dx.doi.org/11299/109020>
- KÖHLER, R., EICHNER, M. (1973): Regionaler Dichteansatz für den Nordteil der DDR, VEB Geophysik. Leipzig. Report
- KOMBRINK, H., DOORNENBAL, J.C., DUIN, E.J.T., DEN DULK, M., VAN GESSEL, S.F., TEN VEEN, J.H., WITMANS, N. (2012): New insights into the geological structure of the Netherlands; results of a detailed mapping project, *Netherlands Journal of Geosciences* 91(4), Cambridge University Press, DOI: <https://doi.org/10.1017/S0016774600000329>
- LAJAUNIE, C., COURRIOUX, G., MANUEL, L. (1997): Foliation Fields and 3D Cartography in Geology: Principles of a Method Based on Potential Interpolation, *Mathematical Geology* 29, Springer, pp. 571-584.
- Landesamt für Bergbau, Energie und Geologie (Hrsg.) (2015): Symbolschlüssel Geologie - Symbole für die Dokumentation geologischer Feld- und Aufschlusdaten: 2 Bd., 535 pp.
- LEHNER, K., ROTHE, K. (1962): Geophysikalische Bohrlochmessungen, Akademie-Verlag, Berlin, Germany, 300p.
- LINDSAY, M.D., AILLÈRES, L., JESSELL, M.W., DE KEMP, E.A., BETTS, P.G. (2012): Locating and quantifying geological uncertainty in three-dimensional models: Analysis of the Gippsland Basin, southeastern Australia. *Tectonophysics* 456-457, pp. 10-27.



- LINGREY, S., & VIDAL-ROYO, O. (2015): Evaluating the quality of bed length and area balance in 2D structural restorations. *Interpretation*, 3(4), <https://doi.org/10.1190/INT-2015-0126.1>
- LÓPEZ-MIR, B. (2019): Cross-section construction and balancing: examples from the Spanish Pyrenees. In: *Developments in Structural Geology and Tectonics Vol. 5*, pp. 3-23, Elsevier.
- LOVERIDGE, M., PARKES, G., HATTON, L. (1987): 3D modelling of migration velocity fields and velocity error zones, *First Break* 5 (8), EAGE, pp. 281-293.
- MITRA, G. (1994). Strain variation in thrust sheets across the Sevier fold-and-thrust belt (Idaho-Utah-Wyoming): Implications for section restoration and wedge taper evolution. *Journal of Structural Geology* 16(4), pp. 585-602.
- MÖNNIG, E., FRANZ, M. & SCHWEIGERT, G. (2018): Der Jura in der Stratigraphischen Tabelle von Deutschland 2016 (STD 2016). *Z. Dtsch. Ges. Geowiss.* 169, 247-266.
- MOORE, W. R., MA, Y. Z., URDEA, J., & BRATTON, T. (2011): Uncertainty analysis in well-log and petrophysical interpretations. In Y. Z. Ma and P. R. La Pointe (eds.), *Uncertainty analysis and reservoir modelling*, AAPG Memoir 96, pp. 17-28.
- MORETTI, I., CALLOT, J. P. (2012). Area, length and thickness conservation: Dogma or reality? *Journal of Structural Geology* 41, pp. 64-75.
- NAGANAWA, S., SUZUKI, M., IKEDA, K., INADA, N., SATO, R. (2018): Modelling of Cuttings Lag Distribution in Directional Drilling to Evaluate Depth Resolution of Mud Logging, *Proceedings of IADC/SPE Drilling Conference and Exhibition, Fort Worth, Texas, Society of Petroleum Engineers (SPE)*, pp. 506-518.
- NOVAKOVA, L., PAVLIS, T. L. (2017): Assessment of the precision of smart phones and tablets for measurement of planar orientations: A case study, *Journal of Structural Geology* 97, pp. 93-103, <https://doi.org/10.1016/j.jsg.2017.02.015>
- O'HAGAN, A., BUCK, C. E., DANESHKHAH, A., EISER, J. R., GARTHWAITE, P. H., JENKINSON, D. J., OAKLEY, J. E., RAKOW, T. (2006): *Uncertain Judgements: Eliciting Experts' Probabilities*. Wiley, New York, 321pp.
- PAKYUZ-CHARRIER, E., GIRAUD, J., OGARKO, V., LINDSAY, M., JESSELL, M. (2018): Drillhole uncertainty propagation for three-dimensional geological modelling using Monte Carlo, *Tectonophysics* 747-748, Elsevier, pp. 16-39, <https://doi.org/10.1016/j.tecto.2018.09.005>
- PAKYUZ-CHARRIER, E., LINDSAY, M., OGARKO, V., GIRAUD, J., JESSELL, M. (2018): Monte Carlo simulation for uncertainty estimation on structural data in implicit 3-D geological modelling, a guide for disturbance distribution selection and parameterization, *Solid Earth* 9, pp. 385-402, DOI: <https://doi.org/10.5194/se-9-385-2018>
- PARKER, R. L. (1973): The rapid calculation of potential field anomalies. *Geophysical Journal International* 31(4), pp. 447-455. <https://dx.doi.org/10.1111/j.1365-246X.1973.tb06513.x>
- PARKES, G., HATTON, L. (1987): Towards a systematic understanding of the effects of velocity model errors on depth and time migration of seismic data, *First Break* 5 (4), EAGE, pp.121-132.
- PLUYMAEKERS, M.D.P., DOORNENBAL, J.C., MIDDELBURG, H. (2017): *Velmod-3.1*, TNO-Report, TNO, <https://www.nlog.nl/en/velmod-31> (last accessed May 2020).



- POLSON, D., CURTIS, A. (2010): Dynamics of uncertainty in geological interpretation, *Journal of the Geological Society London* 167, pp. 5-10, DOI: <https://dx.doi.org/10.1144/0016-76492009-055>
- PUEYO E.L.; IZQUIERDO-LAVALL E.; RODRÍGUEZ-PINTÓ, A., REY MORAL, C.; OLIVA-URCIA, B., CASAS, A.M., CALVÍN, P., AYALA, C., DEL RIO, P., RAMAJO, J., GARCÍA-LOBÓN, J.L., RUBIO, F. (2016). Petrophysical properties in the Iberian Range and surrounding areas (NE Spain): 1-density. *Journal of Maps* 12 (5), pp. 836-844.
- PUEYO, E. L., POCOVÍ, A., MILLÁN, H., SUSSMAN, A. J. (2004): Map-view models for correcting and calculating shortening estimates in rotated thrust fronts using paleomagnetic data. *Orogenic Curvature: Integrating Paleomagnetic and Structural Analyses*, Geological Society of America Special Paper 383, p. 55-71. [https://dx.doi.org/10.1130/0-8137-2383-3\(2004\)383J57:MMFCACJ2.0.CO;2](https://dx.doi.org/10.1130/0-8137-2383-3(2004)383J57:MMFCACJ2.0.CO;2)
- PUEYO, E. L., AYALA, C., IZQUIERDO-LAVALL, E., RUBIO, F. M., SANTOLARIA, P., CLARIANA, P., SOTO, R., REY-MORAL, C., GARCIA-LOBÓN, J. L., ZEHNER, B., ROMÁN-BERDIEL, T., CASAS, A. M., et al. (2021): Optimized 3D reconstruction workflow based on gravimetric, structural and petrophysical data. Deliverable 6.4 of the GeoERA 3DGEO-EU project. Will be available from <https://www.geoera.eu>
- PYRCZ, M. J., DEUTSCH, C. V. (2014): *Geostatistical Reservoir Modeling – Second Edition*, Oxford University Press, 433 pp.
- READING, A., GALLAGHER, K. (2013): Transdimensional change-point modelling as a tool to investigate uncertainty in applied geophysical inference: An example using borehole geophysical logs, *Geophysics* 78 (3), Society of Exploration Geophysicists, pp.WB89-WB99. DOI: <http://doi.org/10.1190/geo2012-0384.1>
- REICHEL, N., EVANS, M., ALLIOLI, F., MAUBORGNE, M. L., NICOLETTI, L., HARANGER, F., ... & RABREI, R. (2012): Neutron-Gamma Density (NGD): Principles, field test results and log quality control of a radioisotope-free bulk density measurement. In SPWLA 53rd Annual Logging Symposium. Society of Petrophysicists and Well-Log Analysts.
- REMY, N., BOUCHER, A., WU, J. (2009): *Applied Geostatistics with SGEMS*, Cambridge University Press, 264 pp.
- SANS, M., VERGÉS, J., GOMIS, E., PARÉS, J. M., SCHIATTARELLA, M., TRAVÉ, A., CALVET, F., SANTANACH, P., DOULCET, A. (2003): Layer parallel shortening in salt-detached folds: constraint on cross-section restoration. *Tectonophysics* 372(1-2), pp. 85-104.
- SCHAAF, A., BOND, C. E., (2019): Quantification of uncertainty in 3-D seismic interpretation: implications for deterministic and stochastic geomodeling and machine learning, *Solid Earth*, 10, pp. 1049-1061, <https://doi.org/10.5194/se-10-1049-2019>
- SCHMIDT, S., GÖTZE, H. J., FICHLER, C., & ALVERS, M. (2010). IGMAS+ – a new 3D gravity, FTG and magnetic modeling software. GEO-INFORMATIK Die Welt im Netz, edited by: Zipf, A., Behncke, K., Hillen, F., and Scheffermeyer, J., Akademische Verlagsgesellschaft AKA GmbH, Heidelberg, Germany, pp. 57-63.
- SCHÖN, J. H. (2015). *Physical properties of rocks: Fundamentals and principles of petrophysics*. Elsevier.



- SCHWEIZER, D., BLUM, P., BUTSCHER, C. (2017): Uncertainty assessment in 3-D geological models of increasing complexity, *Solid Earth* 8, EGU, pp. 517-530, doi: 10.5194/se-8-515-2017
- SHANNON, C. E., WEAVER, W., (1949): The mathematical theory of communication. University of Illinois Press., Urbana, 117 pp.
- SEIGEL, H.O. (1995): A guide to high precision land gravimeter surveys. Scintrex Limited, 122.
- SILER, D. L., HINZ, N., H., FAULDS, J. E., TOBIN, B., BLAKE, K., TIEDEMAN, A., SABIN, A., LAZARO, M., BLANKENSHIP, D., KENNEDY, M., RHODES, G., NORDQUIST, J., HICKMAN, S., GLEN, J., WILLIAMS, C., ROBERTSON-TAIT, A., CALVIN, W., PETTITT, W. (2016): The Geologic Framework of the Fallon FORGE Site, *GRC Transactions* 40, pp. 573 – 584.
- SKEELS, D. C. (1947). Ambiguity in gravity interpretation. *Geophysics* 12(1), 43-56.
- SOARES, A., (1992): Geostatistical estimation of multi-phase structure, *Mathematical Geology* 24, Springer, pp. 149-160.
- STAFLEU, J., MALJERS, D., GUNNINK, J.L., MENKOVIC, A., & BUSSCHERS, F.S. (2011): 3D modelling of the shallow subsurface of Zeeland, The Netherlands. *Netherlands Journal of Geosciences* 90, Cambridge University Press, pp. 293–310.
- STAFLEU, J., DUBELAAR, C.W. (2016): Product Specification Subsurface model GeoTOP. TNO report 2016, R10133, TNO. Available from: <https://www.dinoloket.nl/en/want-know-more>
- STAFLEU, J., MALJERS, D., GUNNINK, J.L. (2021): Visualisation of uncertainty in voxel models of the shallow subsurface of the Netherlands. 82nd EAGE Conference & Exhibition, Extended Abstracts.
- STANĚK, F., FRANĚK, J., JELÍNEK, J. (2019): Evaluation of 3D model uncertainty in geologically complex areas and with heterogeneous data inputs. In: Roland Baumberger (eds.), Abstract volume of the 5th European Meeting on 3D Geological Modelling, May 22nd – 24th, 2019, Bern, Switzerland.
- STIGSSON, M., MUNIER, R. (2013): Orientation uncertainty goes bananas: An algorithm to visualise the uncertainty sample space on stereonet for oriented objects measured in boreholes, *Computers & Geosciences* 56, Elsevier, pp.56-61. DOI: 10.1016/j.cageo.2013.03.001
- SUSSMAN, A. J., PUEYO, E. L., CHASE, C. G., MITRA, G., & WEIL, A. B. (2012). The impact of vertical-axis rotations on shortening estimates. *Lithosphere* 4(5), p. 383-394.
- TARANTOLA, A. (1987): Inverse problem theory, methods for data fitting and model parameter estimation, Elsevier, 613 pp.
- TENZER, R., & GLADKIKH, V. (2014): Assessment of density variations of marine sediments with ocean and sediment depths. The Scientific World Journal, 2014. <https://dx.doi.org/10.1155/2014/823296>
- THORE, P., SHTUKA, A., LECOUR, M., AIT-ETTAJER, T., COGNOT, R. (2002): Structural uncertainties: Determination, management and applications, *Geophysics* 67 (3), pp. 840-852.
- THIELE, S. T., JESSELL, M. W., LINDSAY, M., VITALYI, O., WELLMANN, J. F., PAKYUZ-CHARRIER, E. (2016a): The topology of geology 1: Topological analysis, *Journal of Structural Geology* 91, Elsevier, pp. 27-38. <https://doi.org/10.1016/j.jsg.2016.08.009>



THIELE, S. T., JESSELL, M. W., LINDSAY, M., WELLMANN, J. F., PAKYUZ-CHARRIER, E. (2016b): The topology of geology 2: Topological uncertainty, *Journal of Structural Geology* 91, Elsevier, pp. 74-87. <https://doi.org/10.1016/j.jsg.2016.08.010>

TNO (2021): <https://www.dinoloket.nl/en>; DINOloket, data and information In the Dutch subsurface [last visited June 2021].

TUNB (2021):

TVERSKI, A., KAHNEMAN, D. (1974): Judgment under Uncertainty: Heuristics and Biases. *Science* 185, pp. 1124-1131.

VONDRÁK, I. (2009): Artificial intelligence and neural networks, VŠB-TU Ostrava (in Czech), 139 pp.

WELLMANN, J. F., REGENAUER-LIEB, K. (2012): Uncertainties have a meaning: Information entropy as a quality measure for 3-D geological models, *Tectonophysics* 526-529, Elsevier, pp. 207-216.

WHITTAKER, A., MORTON-THOMPSON, D. (1992): Mudlogging: Drill Cuttings Analysis, In: Morton-Thompson, D., Woods, A. M. (eds.): Development Geology Reference Manual, *AAPG Methods in Exploration Series No 10*, 104-105, AAPG. https://wiki.aapg.org/Mudlogging:_drill_cuttings_analysis

WILSON, C. G., BOND, C. E., SHIPLEY, T. F. (2019): How can geologic decision-making under uncertainty be improved? *Solid Earth*, 10, pp.1469-1488, <https://doi.org/10.5194/se-10-1469-2019>

WITTER, J. B., TRAIOR-GUITTON, W. J., SILER, D. L. (2019): Uncertainty and risk evaluation during the exploration stage of geothermal development: A review, *Geothermics* 78, Elsevier, p.233-242, <https://doi.org/10.1016/j.geothermics.2018.12.011>

WOLF, C.J.M., WARDT, J.P. (1981): Borehole Position Uncertainty - Analysis of Measuring Methods and Derivation of Systematic Error Model, *Journal of Petroleum Technology* 33(12), Society of Petroleum Engineers (SPE), pp.2339-2350. DOI: <https://doi.org/10.2118/9223-PA>

WOODWARD, N. B. (2012): Evaluation, analysis and prediction of geologic structures. *Journal of Structural Geology* 41, p. 76-85.